USGS
science for a changing world

Temperature and Petroleum Generation History of the Wilcox Formation, Louisiana

By Janet K. Pitman and Elisabeth Rowan

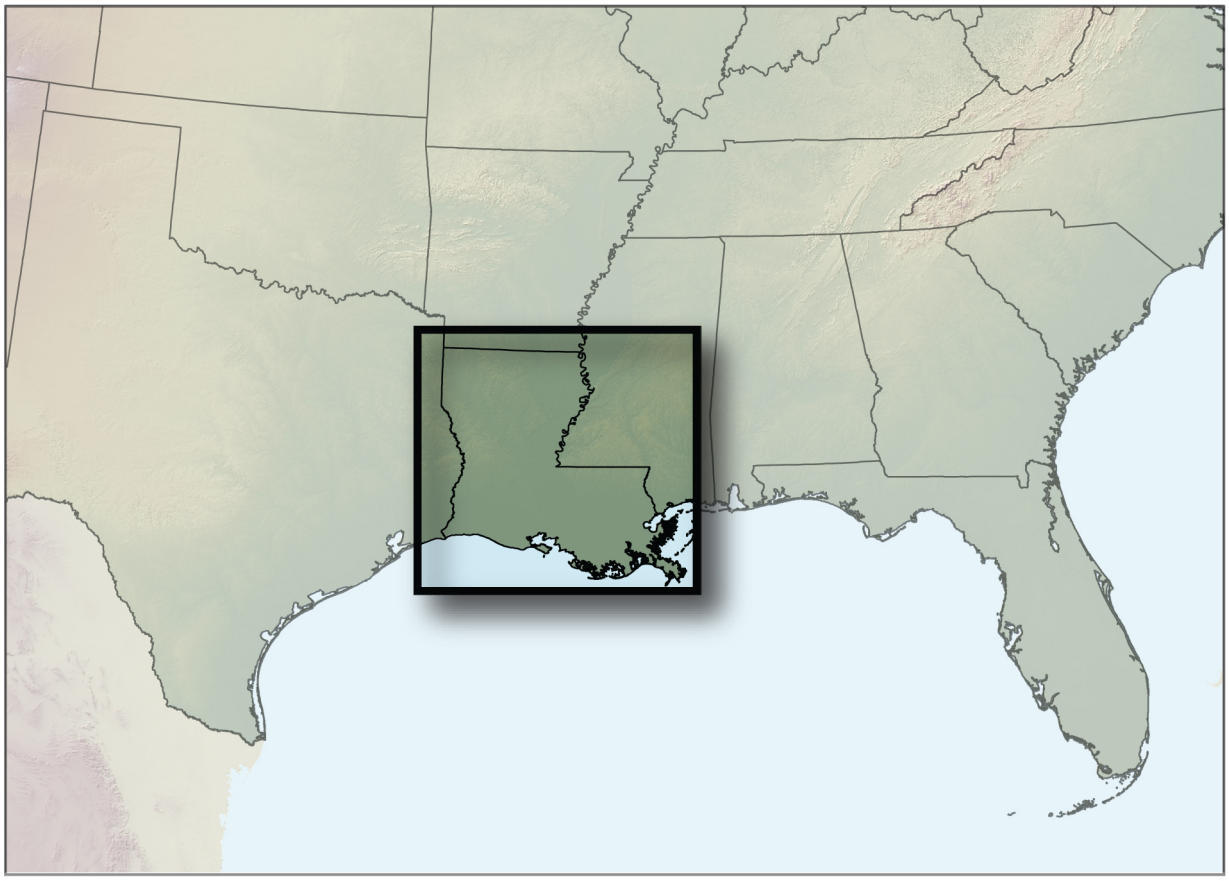

Open-File Report 2012–1046

U.S. Department of the Interior
U.S. Geological Survey

U.S. Department of the Interior
KEN SALAZAR, Secretary

U.S. Geological Survey
Marcia K. McNutt, Director

U.S. Geological Survey, Reston, Virginia: 2012

For product and ordering information:
World Wide Web: http://www.usgs.gov/pubprod
Telephone: 1–888–ASK–USGS

For more information on the USGS—the Federal source for science about the Earth,
its natural and living resources, natural hazards, and the environment:
World Wide Web: http://www.usgs.gov
Telephone: 1–888–ASK–USGS

Suggested citation:
Pitman, J.K., and Rowan, Elisabeth, 2012, Temperature and petroleum generation history of the Wilcox Formation, Louisiana: U.S. Geological Survey Open-File Report 2012–1046, 51 p.

Contents

Figures

Tables

Abbreviations Used in This Report

≈	nearly equal to
ft	foot or feet
g	gram
Ma	mega-annum; million years ago
mD	millidarcy
mg HC/g TOC	milligrams of hydrocarbon per gram of total organic carbon
mW/m^2	milliwatt per square meter
m.y.	million years
R_o	vitrinite reflectance
T_{max}	temperature of maximum hydrocarbon generation
TOC	total organic carbon
TPS	total petroleum system
USGS	U.S. Geological Survey

Temperature and Petroleum Generation History of the Wilcox Formation, Louisiana

By Janet K. Pitman and Elisabeth Rowan

Abstract

A one-dimensional petroleum system modeling study of Paleogene source rocks in Louisiana was undertaken in order to characterize their thermal history and to establish the timing and extent of petroleum generation. The focus of the modeling study was the Paleocene and Eocene Wilcox Formation, which contains the youngest source rock interval in the Gulf Coast Province. Stratigraphic input to the models included thicknesses and ages of deposition, lithologies, amounts and ages of erosion, and ages for periods of nondeposition. Oil-generation potential of the Wilcox Formation was modeled using an initial total organic carbon of 2 weight percent and an initial hydrogen index of 261 milligrams of hydrocarbon per grams of total organic carbon. Isothermal, hydrous-pyrolysis kinetics determined experimentally was used to simulate oil generation from coal, which is the primary source of oil in Eocene rocks. Model simulations indicate that generation of oil commenced in the Wilcox Formation during a fairly wide age range, from 37 million years ago to the present day. Differences in maturity with respect to oil generation occur across the Lower Cretaceous shelf edge. Source rocks that are thermally immature and have not generated oil (depths less than about 5,000 feet) lie updip and north of the shelf edge; source rocks that have generated all of their oil and are overmature (depths greater than about 13,000 feet) are present downdip and south of the shelf edge. High rates of sediment deposition coupled with increased accommodation space at the Cretaceous shelf margin led to deep burial of Cretaceous and Tertiary source rocks and, in turn, rapid generation of petroleum and, ultimately, cracking of oil to gas.

Introduction

Petroleum system modeling of Paleogene source rocks was undertaken in Louisiana and Texas as part of the U.S. Geological Survey's assessment of oil and gas resources in Tertiary rocks of the Gulf Coast (U.S. Geological Survey, 2007) (fig. 1). The source rock interval was modeled in order to characterize its thermal history and to establish the timing and extent of petroleum generation in the depositional area. Characterizing the timing and extent of generation in these rocks is critical in defining the total petroleum system (TPS) and its undiscovered oil and gas resources. The TPS, as defined in the U.S. Geological Survey (USGS) Gulf Coast Assessment (U.S. Geological Survey, 2007), extends from the Texas-Mexico border on the west to Florida on the east. The northern limit corresponds to the Cretaceous rock outcrop and the southern limit is undefined in Federal waters.

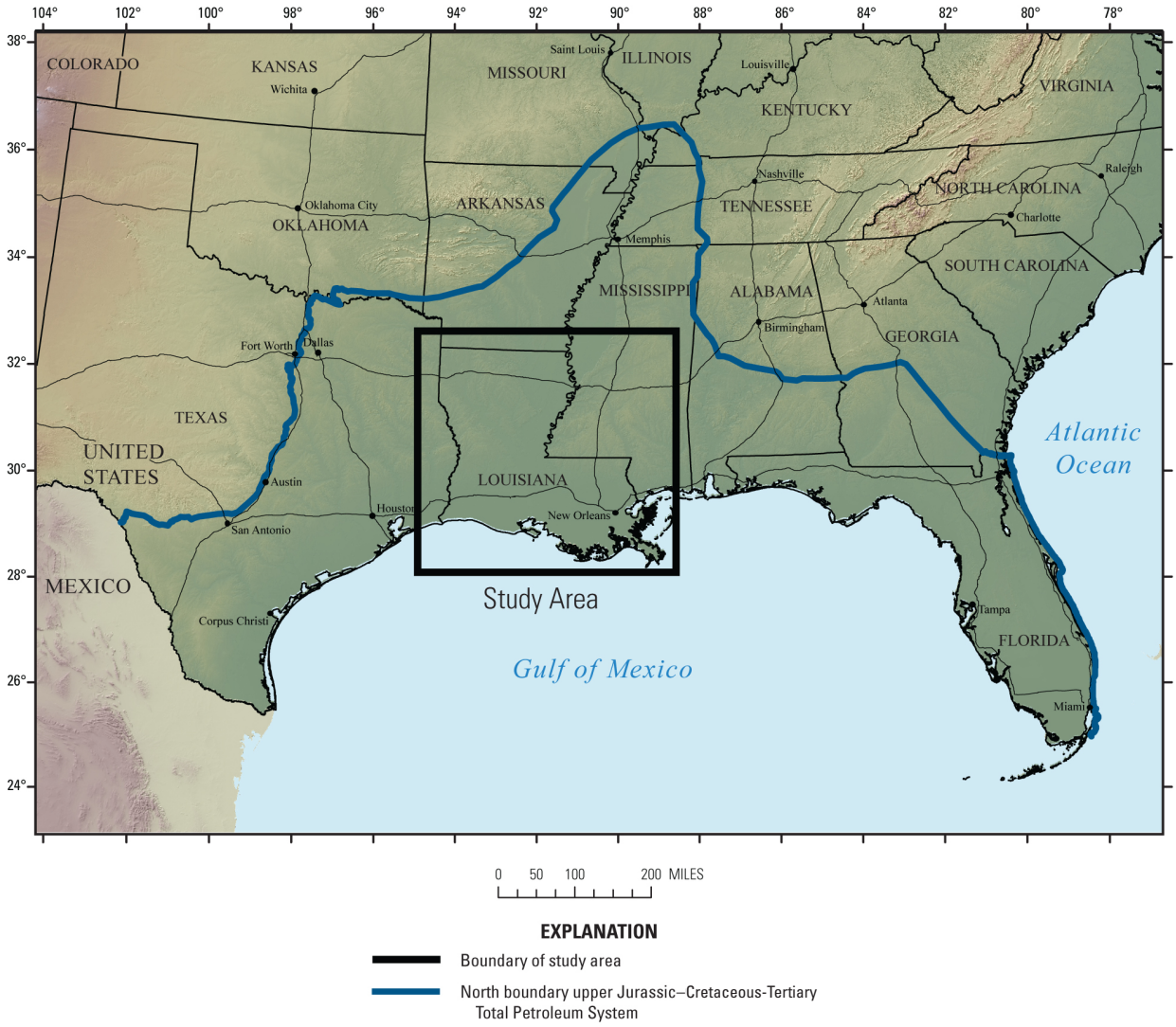

Figure 1. United States Gulf Coast showing part of the Upper Jurassic–Cretaceous–Tertiary Composite Total Petroleum System.

The area of interest in this study is primarily Louisiana (fig. 1). The tectonic and depositional histories of Cenozoic rocks in the Gulf Coast region have been reviewed extensively (for example, Salvador, 1987, 1991) and are discussed only briefly in this report. Mesozoic and Cenozoic strata were deposited as part of a seaward-dipping wedge of sediments that accumulated in differentially subsiding basins on the passive margin of the North American craton (Martin, 1978). Mesozoic fine-grained carbonates and Cenozoic clastic rocks ranging from sandstone to siltstone and shale compose the stratigraphic section in Louisiana; Jurassic salt also is an important lithologic constituent. Paleoenvironments were predominantly fluvial and deltaic, with some turbidite deposition occurring locally in deep marine environments. The Mesozoic-Cenozoic section increases in thickness from north to south toward the coastal areas (Salvador, 1991); however, much of the interval has not been penetrated by drilling owing to deep burial depths and high pore-fluid pressures.

The focus of the modeling study is the Paleocene and Eocene Wilcox Formation, which contains the youngest source rock interval in the Gulf Coast Province. One-dimensional petroleum system models were developed for 28 wells in northern and central Louisiana (fig. 2). The wells that were selected for modeling penetrated the lower part of the Paleogene section and have downhole temperature data for model calibration. Models were generated using IES Integrated Exploration Systems PetroMod (v. 9) software. An important aspect of the modeling study involved determining the timing of oil generation in the Wilcox by using hydrous-pyrolysis kinetic parameters. Thermal maturity estimates and timing of petroleum generation based on bulk Rock-Eval kinetics are not always consistent with the burial-thermal history of a region. However, hydrous-pyrolysis kinetic parameters provide optimal results when they are used to model oil generation in sedimentary basins because they yield generative histories that are geologically reasonable (Hunt and others, 1991; Ruble and others, 2001; Lewan and Ruble, 2002). Interpretations from petroleum system models combined with knowledge of a basin's evolution provide important constraints for estimating potential undiscovered petroleum accumulations in unexplored Paleogene and Neogene reservoirs.

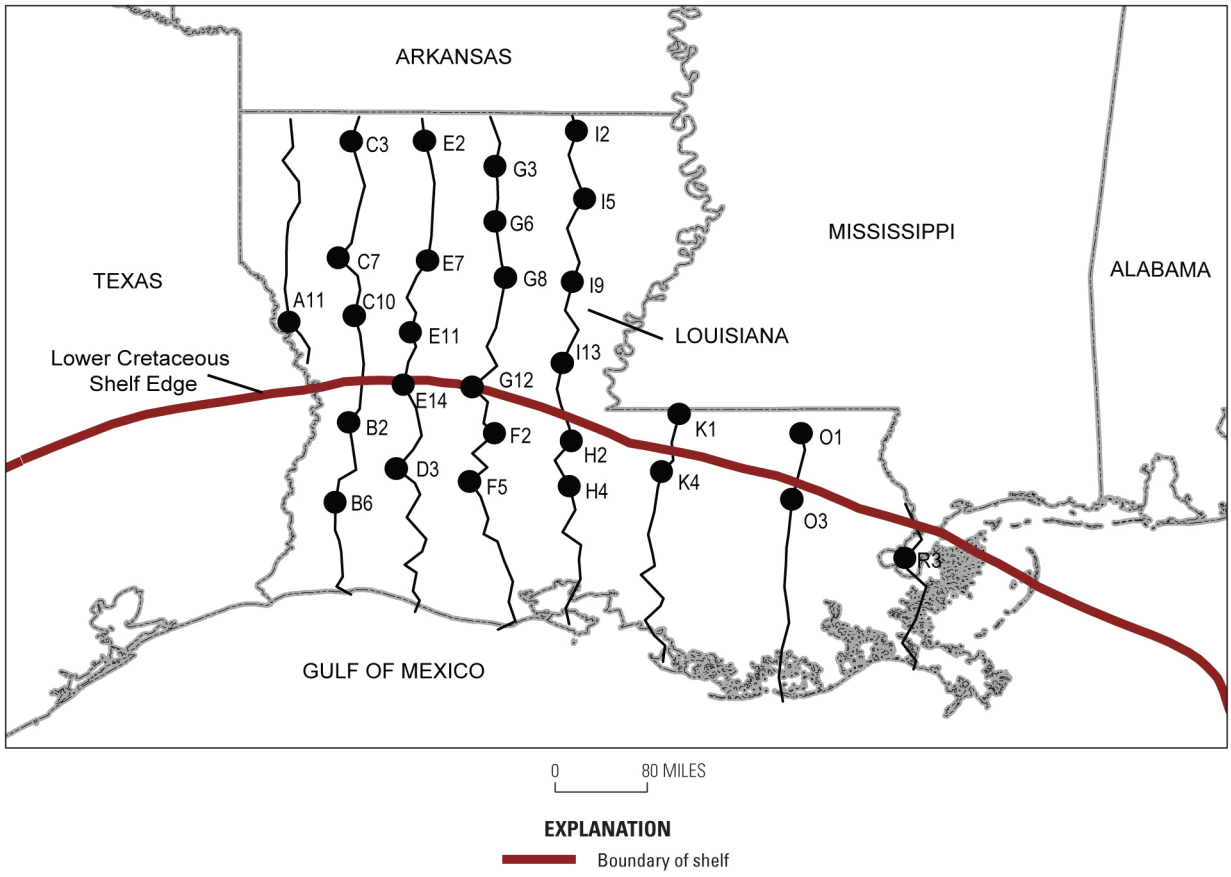

Figure 2. Locations of cross sections and wells in Louisiana study area.

Gulf Coast Mesozoic and Cenozoic Rock Units

Eight north-south-trending cross sections (Bebout and Gutierrez, 1982, 1983; Eversull, 1984) provided the stratigraphic framework of Gulf Coast Mesozoic and Cenozoic rock units for one-dimensional model simulations. In order to compare our model results for Louisiana with results from a similar study of Texas (Elisabeth Rowan, unpub. data, 2007), the Mesozoic and Cenozoic section was subdivided on the basis of geologic age into 20 chronostratigraphic units recognized in both states. The size of the geographic area and complex stratigraphy required that several units be combined. The simplified stratigraphic framework and nomenclature used to define the model units are summarized in figure 3.

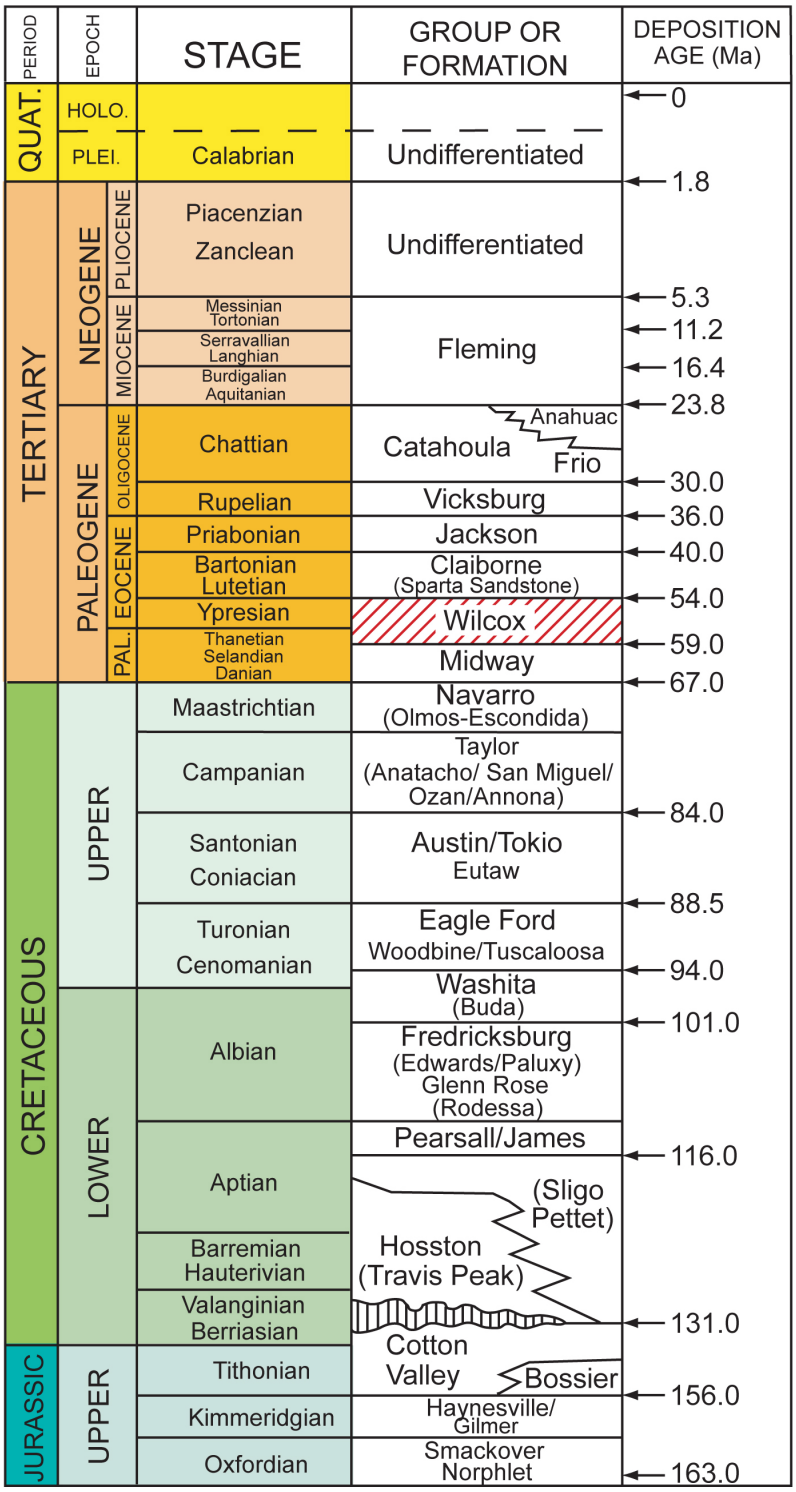

Figure 3. Stratigraphic column of Gulf Coast region showing group or formation used in the modeling study. Event ages from Salvador and Muneton (1991); Wilcox Formation shown in red hachures. Quat., Quaternary; Holo., Holocene; Plei., Pleistocene; Pal., Paleocene.

Input to the models includes stratigraphic thicknesses and ages of deposition, lithologies, amounts and ages of erosion, and ages of periods of nondeposition. Thicknesses of chronostratigraphic units and amounts of erosion were estimated from the well-log cross sections (Bebout and Gutierrez, 1982, 1983, 1984) and the geologic ages assigned to each depositional and erosional event were from the Gulf of Mexico Basin stratigraphic correlation chart (Salvador and Muneton, 1991). On the basis of regional stratigraphic trends (Morton and others, 1990; Stoudt and others, 1990a,b; Salvador, 1991), lithologies were defined as end-member rock types, or as mixtures to account for variations in lithofacies within a unit (table 1). The physical and thermal properties (compaction, porosity, thermal conductivity, heat capacity) of the defined lithologies and lithology mixes were assigned default values by the software. Overpressured zones and their possible effects on source rock maturity were not included in the model simulations.

Table 1. Formation lithologies and physical and thermal properties as defined in models of Louisiana wells.

[ss, sandstone; slt, siltstone; sh, shale; carb, carbonate; evap, evaporite; T-cond., thermal conductivity; kg/m^3, kilogram per cubic meter; W/mK, watts per meter kelvin; kcal/kg/K, kilocalories per kilogram per kelvin]

Model	Lithology	Density	Initial	T-cond.	T-cond.	T-cond.	Heat capacity	Heat capacity	Permeability	Permeability	Permeability
Unit			porosity	at 20° C	at 100° C	Anisotropy	at 20° C	at 100° C	at 5% porosity	at 75% porosity	anisotropy
Name	(percent)	(Kg/m**3)	(fraction)	(W/mK)	(W/mK)	(Fraction)	(kcal/kg/K)	(kcal/kg/K)	(log mD)	(log mD)	(log)
PLEISTOCENE	65 SS/30 SLT/05 SH	2,664.6	0.47	2.77	2.42	1.18	0.187	0.221	-1.13	5.80	1.44
PLIOCENE	50 SS/40 SLT/10 SH	2,666.8	0.50	2.61	2.32	1.22	0.191	0.227	-2.05	4.40	1.60
UPPER MIOCENE	20 SS/60 SLT/20 SH	2,671.2	0.55	2.30	2.13	1.30	0.199	0.239	-3.90	1.60	1.92
MIDDLE MIOCENE	15 SS/55 SLT/30 SH	2,672.6	0.57	2.24	2.09	1.33	0.201	0.242	-4.25	1.05	2.02
LOWER MIOCENE	20 SS/55 SLT/25 SH	2,671.6	0.55	2.30	2.12	1.31	0.199	0.239	-3.92	1.55	1.95
FRIO	15 SS/55 SLT/30 SH	2,672.6	0.57	2.24	2.09	1.33	0.201	0.242	-4.25	1.05	2.02
VICKSBURG	20 SS/55 SLT/25 SH	2,671.6	0.55	2.30	2.12	1.31	0.199	0.239	-3.92	1.55	1.95
JACKSON	15 SS/50 SLT/35 SH	2,673.0	0.57	2.23	2.08	1.34	0.202	0.243	-4.28	1.00	2.04
CLAIBORNE	10 SS/35 SLT/55 SH	2,675.2	0.60	2.15	2.02	1.39	0.205	0.248	-4.68	0.35	2.19
WILCOX	20 SS/60 SLT/20 SH	2,671.2	0.55	2.30	2.13	1.30	0.199	0.239	-3.90	1.60	1.92
MIDWAY	10 SLT/90 SH	2,679.2	0.64	2.00	1.92	1.48	0.212	0.256	-5.45	-0.90	2.45
NAVARRO	15 SLT/65 SH/10 CARB/10 CHALK	2,683.8	0.60	2.18	2.05	1.39	0.208	0.249	-4.85	0.98	2.15
AUSTIN	5 SLT/5 SH/90 CHALK	2,697.6	0.65	2.77	2.46	1.13	0.198	0.228	-1.43	2.65	1.22
EAGLEFORD	10 SLT/90 SH	2,679.2	0.64	2.00	1.92	1.48	0.212	0.256	-5.45	-0.90	2.45
TUSCALOOSA	35 SS/20 SLT/45 SH	2,671.4	0.55	2.41	2.19	1.32	0.198	0.238	-3.13	2.70	1.91
WASHITA	5 SLT/30 SH/65 CARB	2,699.1	0.38	2.54	2.34	1.23	0.201	0.234	-4.66	8.31	1.56
FREDRICKSBURG	5 SLT/10 SH/75 CARB/10 EVAP	2,688.1	0.28	2.90	2.60	1.14	0.197	0.226	-5.59	8.24	1.18
SLIGO	25 SS/15 SLT/15 SH/45 CARB	2,687.3	0.39	2.67	2.40	1.19	0.194	0.228	-3.24	8.06	1.45
COTTON VALLEY	15 SS/40 SLT/20 SH/20 CARB/5 EVAP	2,672.8	0.47	2.52	2.30	1.26	0.198	0.235	-4.60	3.00	1.69
SMACKOVER	5 SS/95 CARB	2,707.5	0.25	2.84	2.56	1.10	0.194	0.222	-3.99	13.04	1.10

*; Thermal Conductivity

Source Rock Properties Used in Petroleum System Models

Source rock properties defined in the petroleum system models include initial richness, represented as total organic carbon (TOC), and initial petroleum generation potential represented by hydrogen index. Kinetic parameters that simulate the thermal cracking of kerogen to oil (or gas) also were defined for the source interval. Rock-Eval data indicate that coaly shales in the Wilcox Formation presently have TOC contents ranging from 0.97 to 4.00 weight percent and hydrogen indices between 160 to 255 milligrams of hydrocarbon per gram total organic carbon (mg HC/g TOC) (Sassen and others, 1988). Source-rock generation potential was modeled using an initial TOC of 2 weight percent and an initial hydrogen index of 261 mg HC/g TOC. Isothermal, hydrous-pyrolysis kinetics determined experimentally were used to simulate oil generation of the Wilcox (M.D. Lewan, written commun., 2007). Hydrous-pyrolysis kinetics assumes that the process of generating petroleum from kerogen is a series of parallel first-order reactions. Those reactions are based on discrete or continuous Gaussian distributions of activation energies, and they result in a set of transformation ratios that represent the decimal fraction of the petroleum reaction completed. In the example shown in figure 4, a transformation ratio equal to zero indicates no reaction, and a ratio of one indicates 100 percent reaction. Transformation ratios also can be used to estimate the timing of generation. The onset, peak, and end of oil generation in the present study are defined by ratios of 0.05, 0.50, and 0.95, respectively.

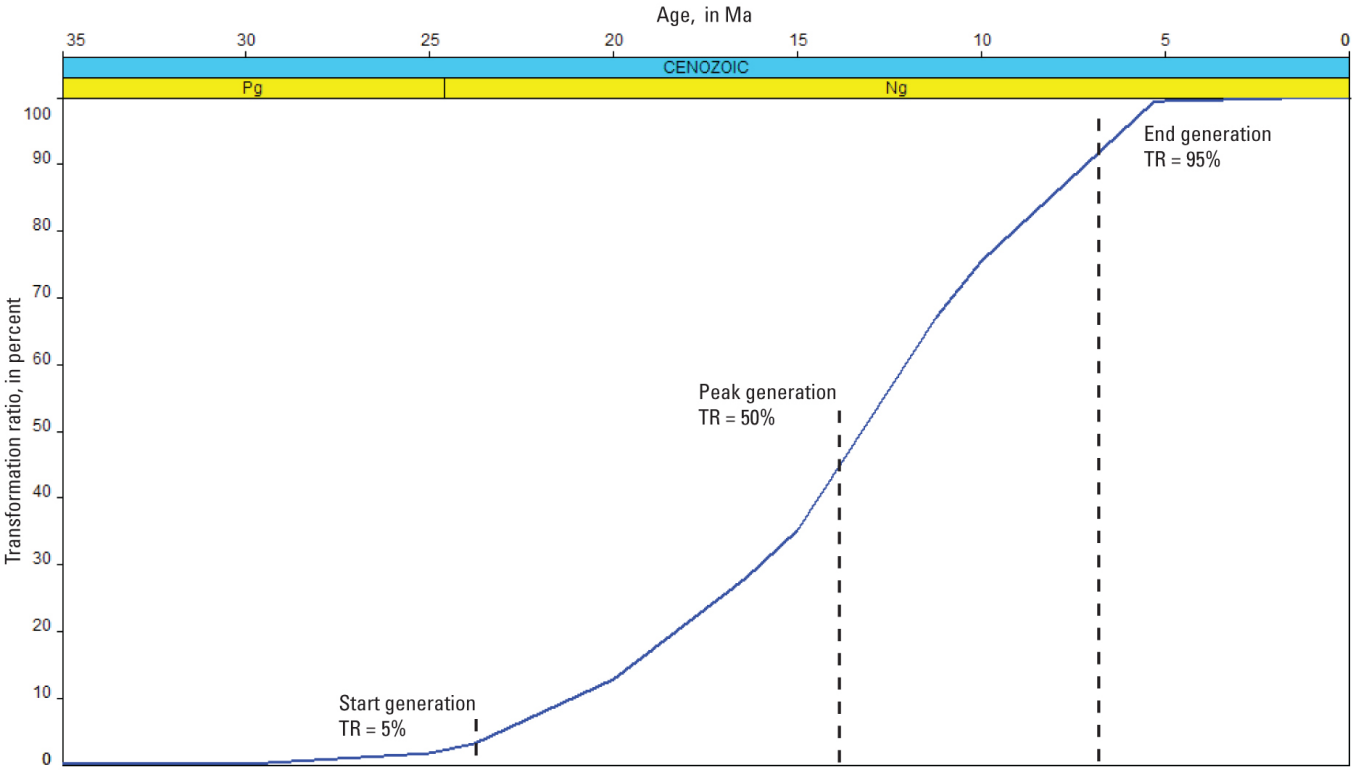

Figure 4. Hypothetical transformation ratio curve depicting start, peak, and end of oil generation. Transformation ratios (TR) computed from hydrous pyrolysis kinetics. Ma, mega-annum.

Model simulations of gas generation in the Wilcox Formation assume that a component of Type III organic matter enriched in oxygen is present locally in the source rock interval. In this study, gas refers to thermogenic gas generated from kerogen; biogenic gas, which can be generated at any time during shallow burial, was not considered in the modeling. Unlike the generation of oil, generation of gas cannot be related to specific transformation ratios due to the lack of acceptable kinetic models for gas-prone source rocks (Roberts and others, 2004). Consequently, the timing of gas generation was determined on the basis of the empirical relation between vitrinite reflectance (R_o) and the gas-generation kinetics for waxy Type III kerogen (Pepper and Corvi, 1995) and North Dakota lignite (Tang and others, 1996). Experimental studies (Tang and others, 1996) indicate that generation of gas from humic coals and organic matter with Type III kerogen begins at about 0.5 percent R_o and reaches a peak between 0.8 and 1.0 percent R_o. The end of gas generation in Type III kerogen corresponds to values between 1.8 and 2.0 percent R_o (Kotarba and Lewan, 2004).

Boundary Conditions Used in Petroleum System Models

Sediment-water-interface temperatures and paleoheat flow are boundary conditions that must be defined in the models. Temperatures at the sediment-water interface through time were calculated within PetroMod by an algorithm (Wygrala, 1989) that relates mean paleosurface temperature and geologic age as a function of plate tectonic reconstructions at present-day latitudes (fig. 5).

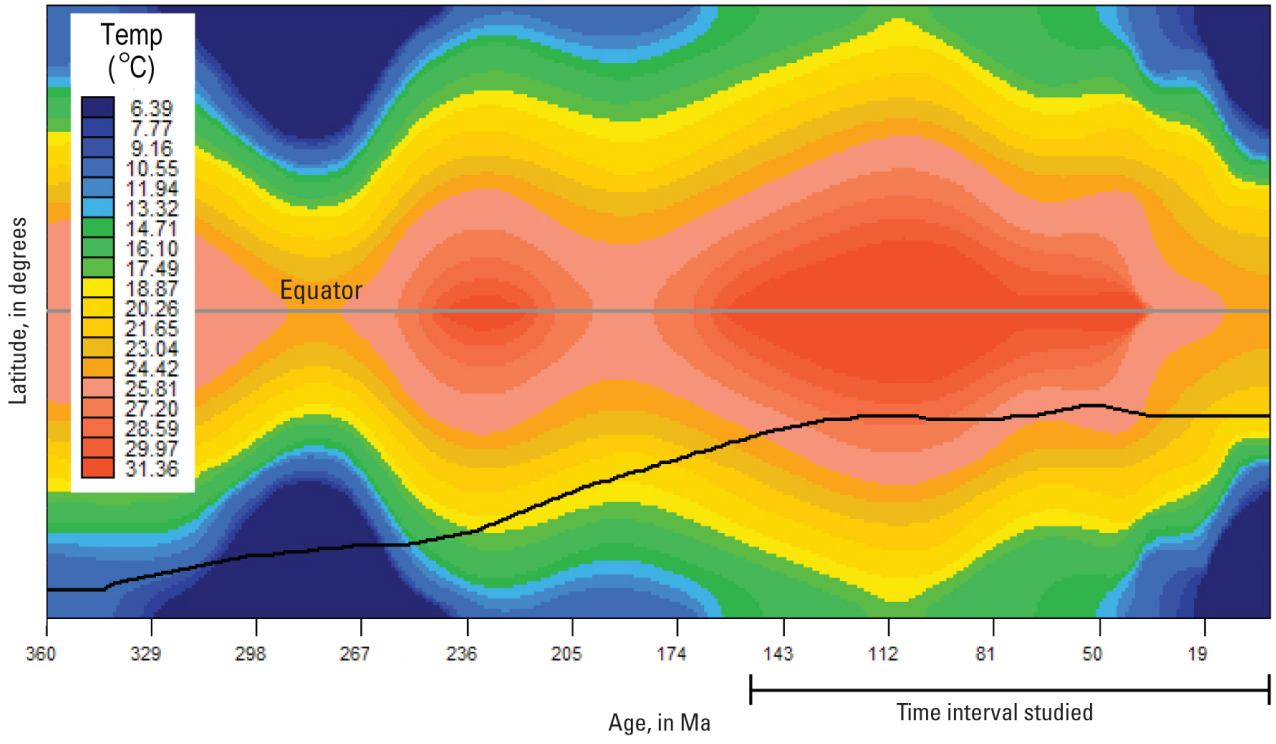

Figure 5. Global mean surface temperature as a function of latitude and geologic age (from Wygrala, 1989). Position of solid dark line within the interval labeled "Time interval studied" corresponds to sediment-water-interface temperature during deposition of sediments in Louisiana (North America, ≈30° south latitude, present day). Ma, mega-annum.

Heat flow is defined at the base of the sedimentary column; it is an important parameter controlling a basin's present and past thermal regime. Typically, heat flow is determined on the basis of knowledge of the geothermal gradient and thermal conductivity of the rock units. Radiogenic heat production may contribute to the temperature distribution in the sedimentary section (Keen and Lewis, 1982; McKenna and Sharp, 1998; Negraru and others, 2004), but the importance of such a source is controversial (Hermanrud, 1993) because the magnitude of radiogenic heat is difficult to determine. Therefore, heat originating only from basement rocks was incorporated in the models. All heat flow was assumed to be steady state. In this study, initial heat flow values were defined at each well location by use of a surficial heat flow map (Blackwell and Richards, 2004), and those values then were optimized until they produced temperature-depth profiles that fit uncorrected and corrected bore-hole temperature measurements (fig. 6). The temperature difference in the majority of profiles (fig. 6) reaches a maximum (20–30°F) at burial depths of approximately 12,000 feet (ft). In the Wilcox Formation, the difference between uncorrected and corrected temperatures generally is less than 20°F, which does not significantly affect the model results. The present geothermal gradients of the temperature-corrected profiles, if we assume an average surface temperature of 68°F, range from 1.3 to 2.1°F per 100 feet (°F/100 ft). Calibrated heat flow values based on uncorrected and corrected temperature measurements range from 34 to 71 milliwatts per square meter (mW/m^2) (average 46 mW/m^2) and 44 to 75 mW/m^2 (average 55 mW/m^2), respectively. The average heat flow values based on corrected temperatures fall within the range of values (37–77 mW/m^2) previously reported for the onshore Gulf Coast (Smith and others, 1981; Nunn and Sassen, 1986).

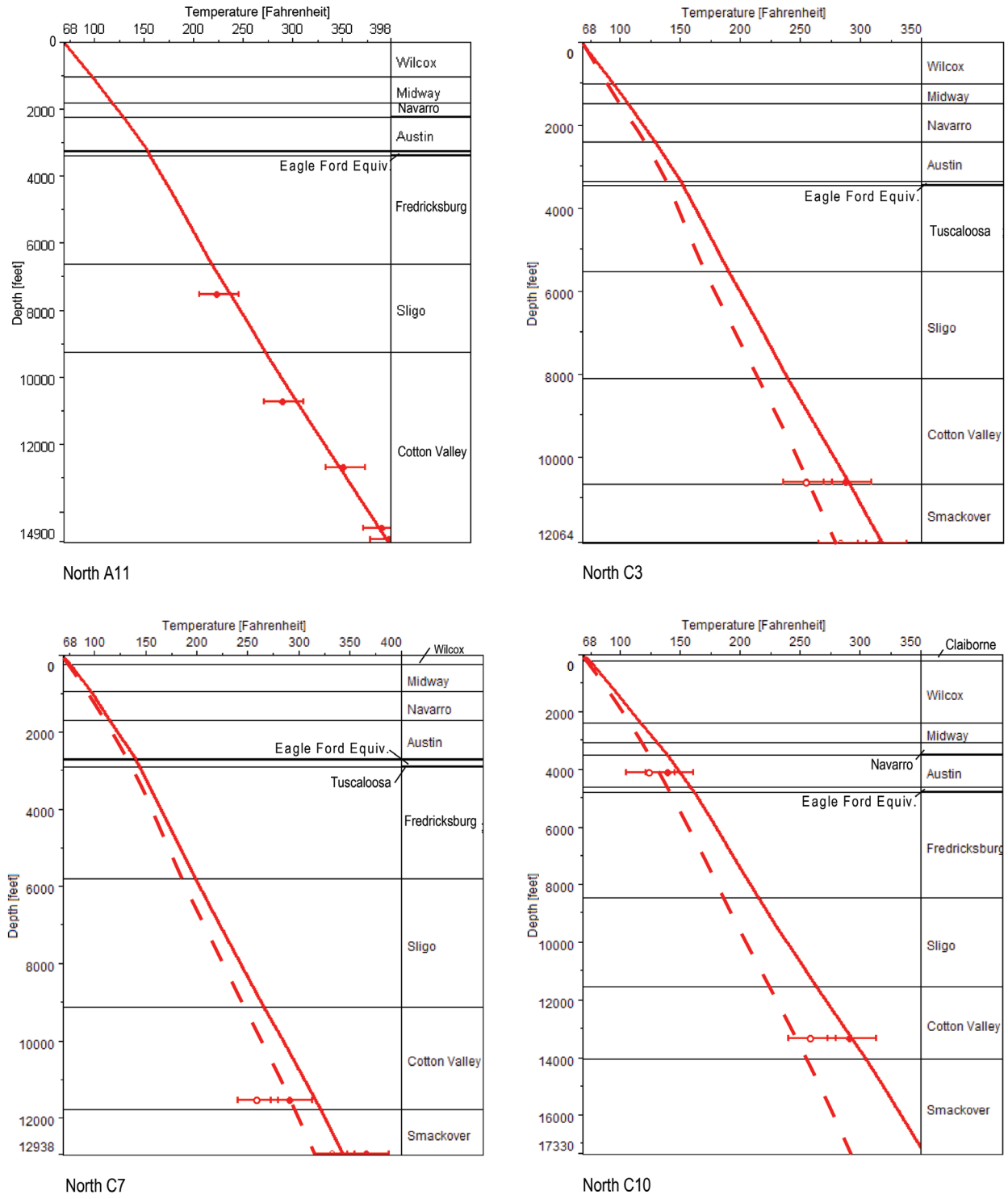

Figure 6. Calculated temperature profiles of modeled wells; see figure 2 for well locations. Dashed-line profiles based on uncorrected reservoir and bottom-hole temperatures (open circles); solid-line profiles computed from corrected bore-hole temperatures (closed circles). Error bars for temperature data are ±20°F. Corrected and uncorrected temperatures are reported on the cross sections used in the study.

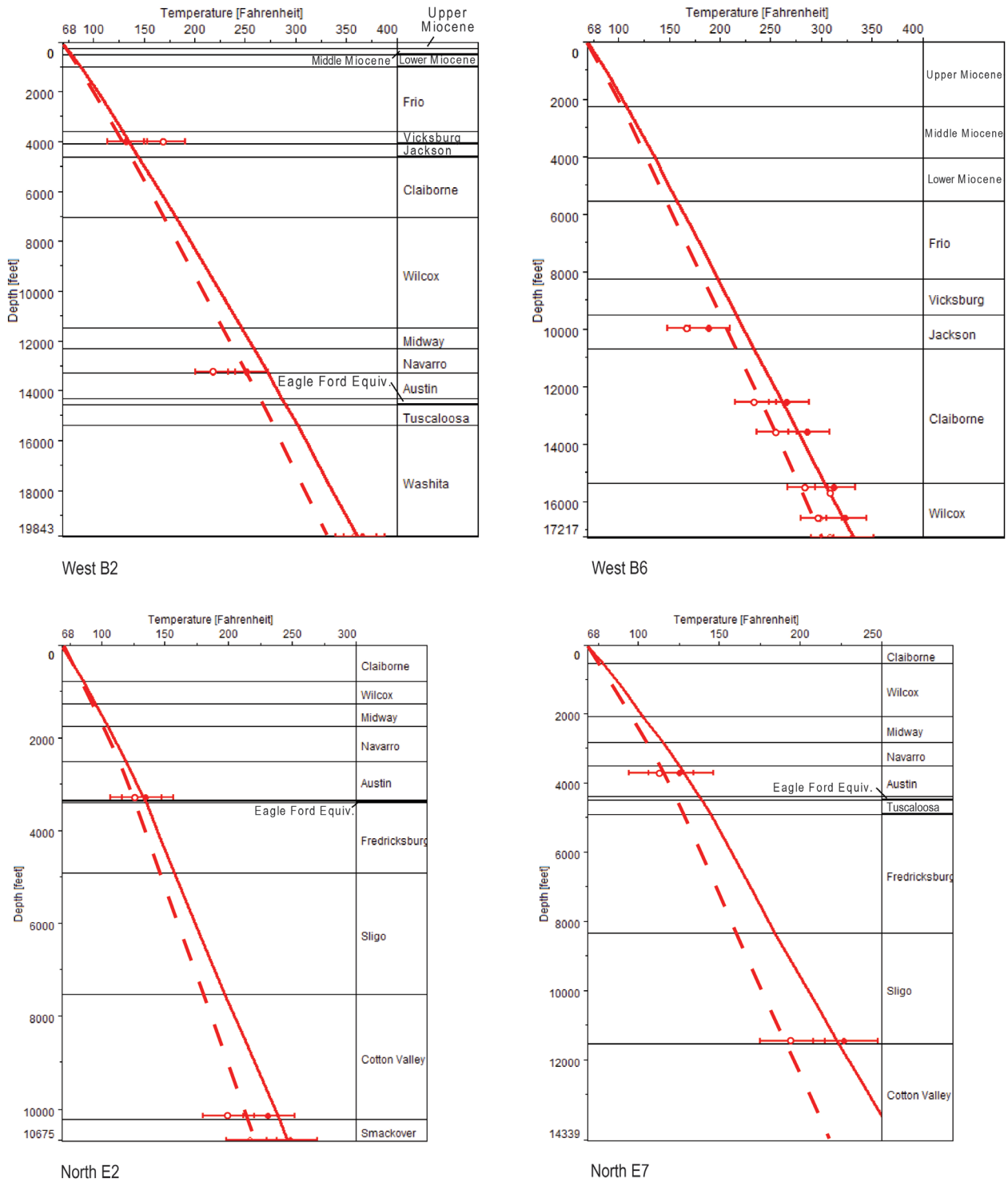

Figure 6. Calculated temperature profiles of modeled wells; see figure 2 for well locations. Dashed-line profiles based on uncorrected reservoir and bottom-hole temperatures (open circles); solid-line profiles computed from corrected bore-hole temperatures (closed circles). Error bars for temperature data are ±20°F. Corrected and uncorrected temperatures are reported on the cross sections used in the study.—Continued

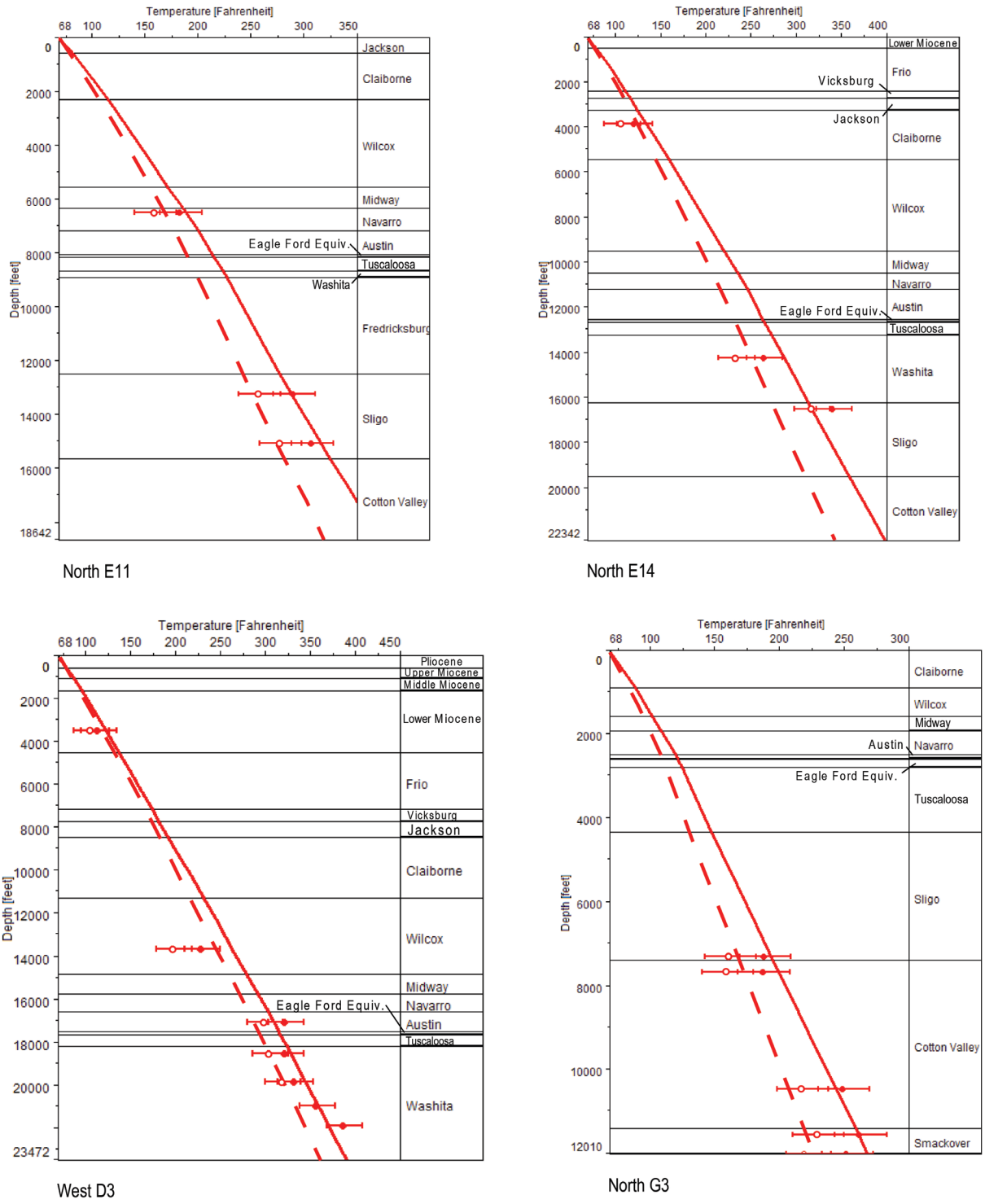

Figure 6. Calculated temperature profiles of modeled wells; see figure 2 for well locations. Dashed-line profiles based on uncorrected reservoir and bottom-hole temperatures (open circles); solid-line profiles computed from corrected bore-hole temperatures (closed circles). Error bars for temperature data are ±20°F. Corrected and uncorrected temperatures are reported on the cross sections used in the study.—Continued

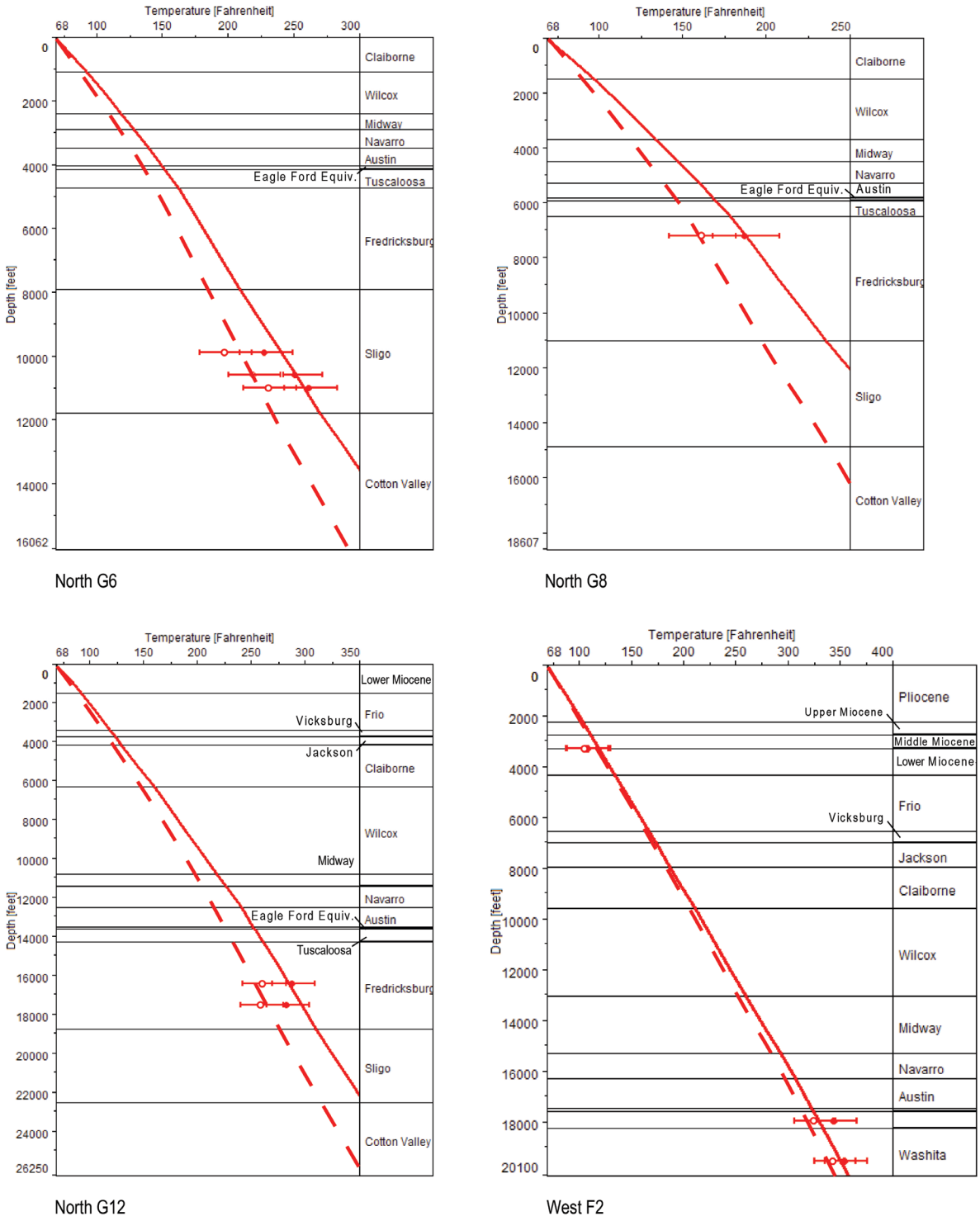

Figure 6. Calculated temperature profiles of modeled wells; see figure 2 for well locations. Dashed-line profiles based on uncorrected reservoir and bottom-hole temperatures (open circles); solid-line profiles computed from corrected bore-hole temperatures (closed circles). Error bars for temperature data are ±20°F. Corrected and uncorrected temperatures are reported on the cross sections used in the study.—Continued

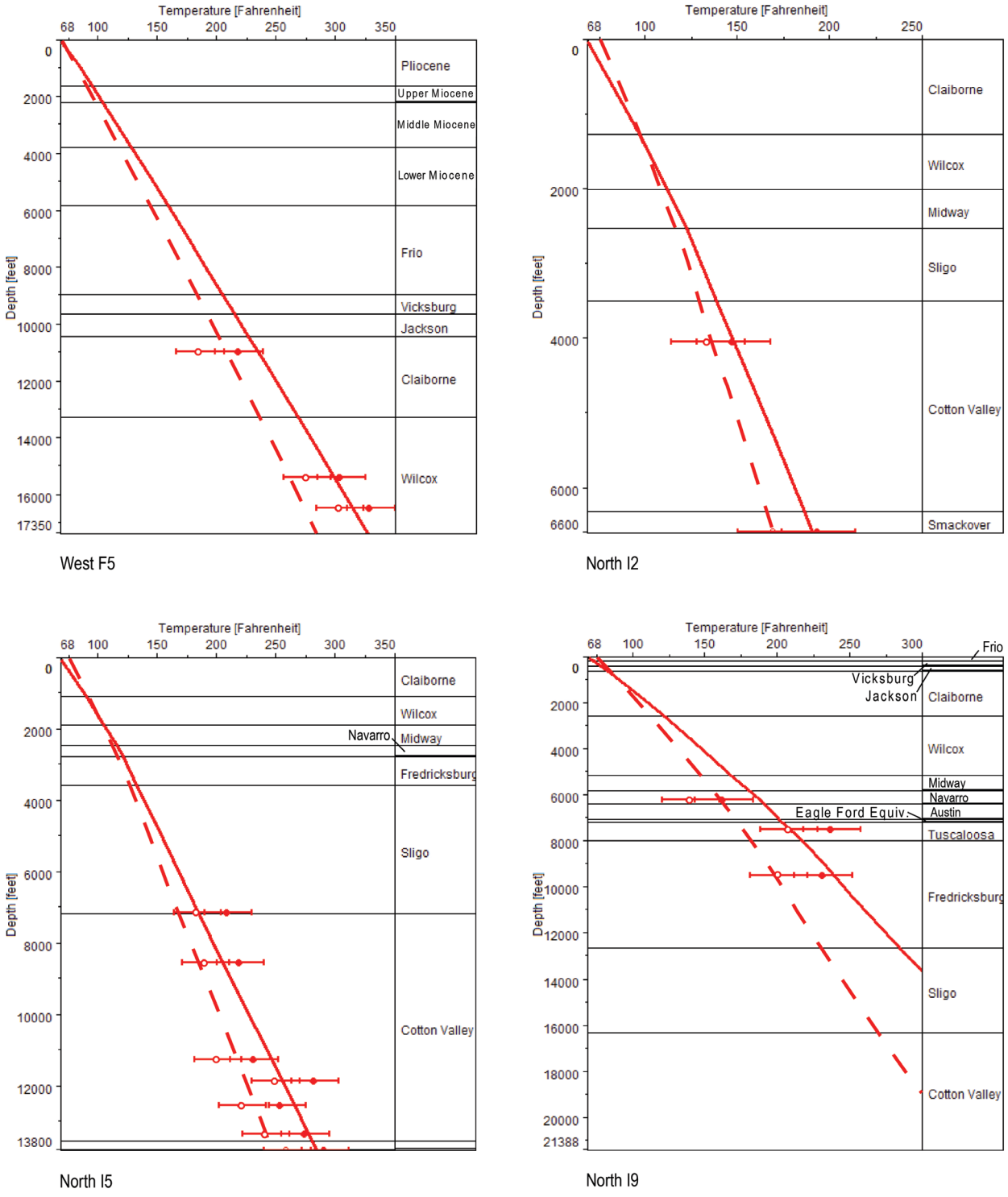

Figure 6. Calculated temperature profiles of modeled wells; see figure 2 for well locations. Dashed-line profiles based on uncorrected reservoir and bottom-hole temperatures (open circles); solid-line profiles computed from corrected bore-hole temperatures (closed circles). Error bars for temperature data are ±20°F. Corrected and uncorrected temperatures are reported on the cross sections used in the study.—Continued

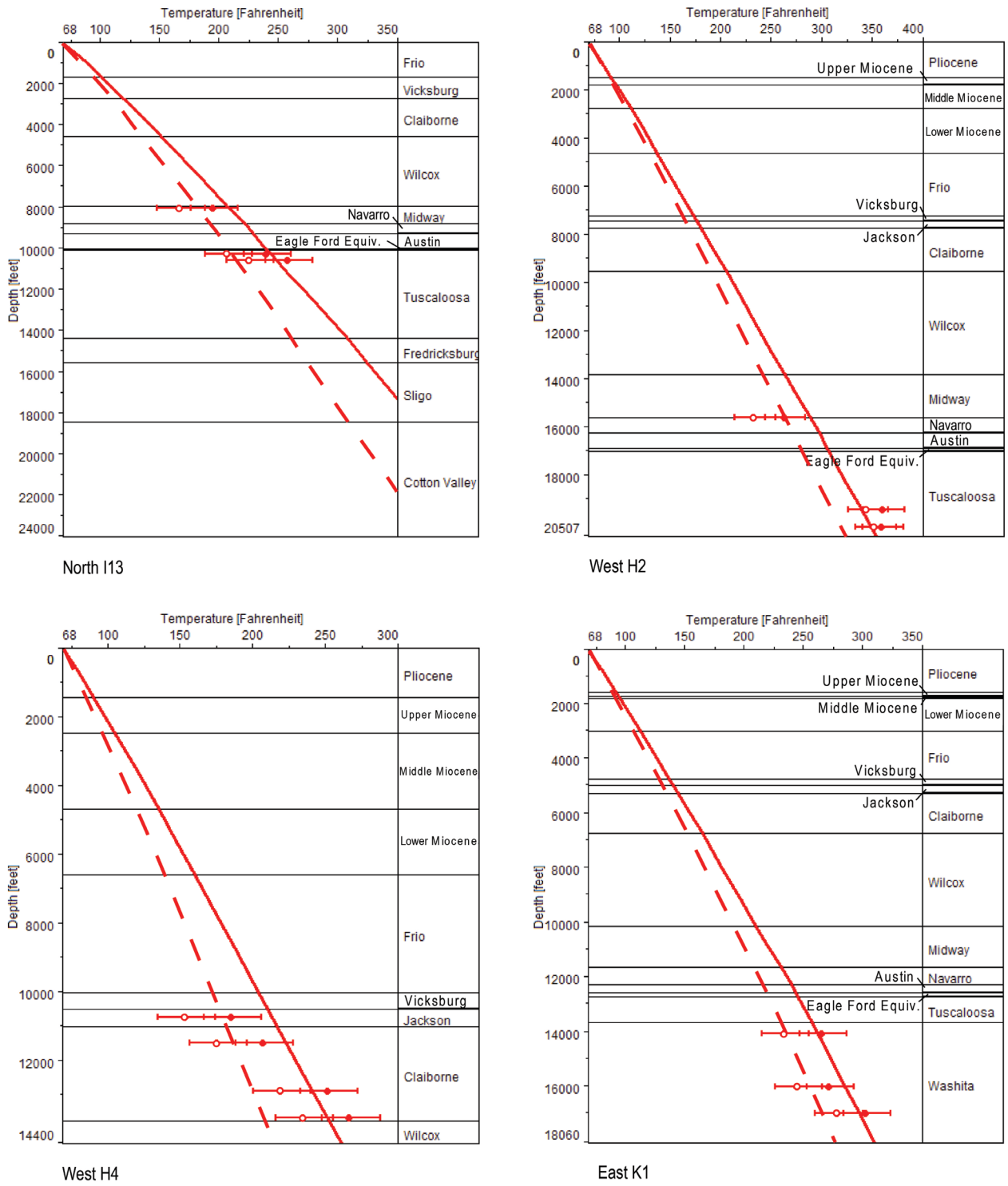

Figure 6. Calculated temperature profiles of modeled wells; see figure 2 for well locations. Dashed-line profiles based on uncorrected reservoir and bottom-hole temperatures (open circles); solid-line profiles computed from corrected bore-hole temperatures (closed circles). Error bars for temperature data are ±20°F. Corrected and uncorrected temperatures are reported on the cross sections used in the study.—Continued

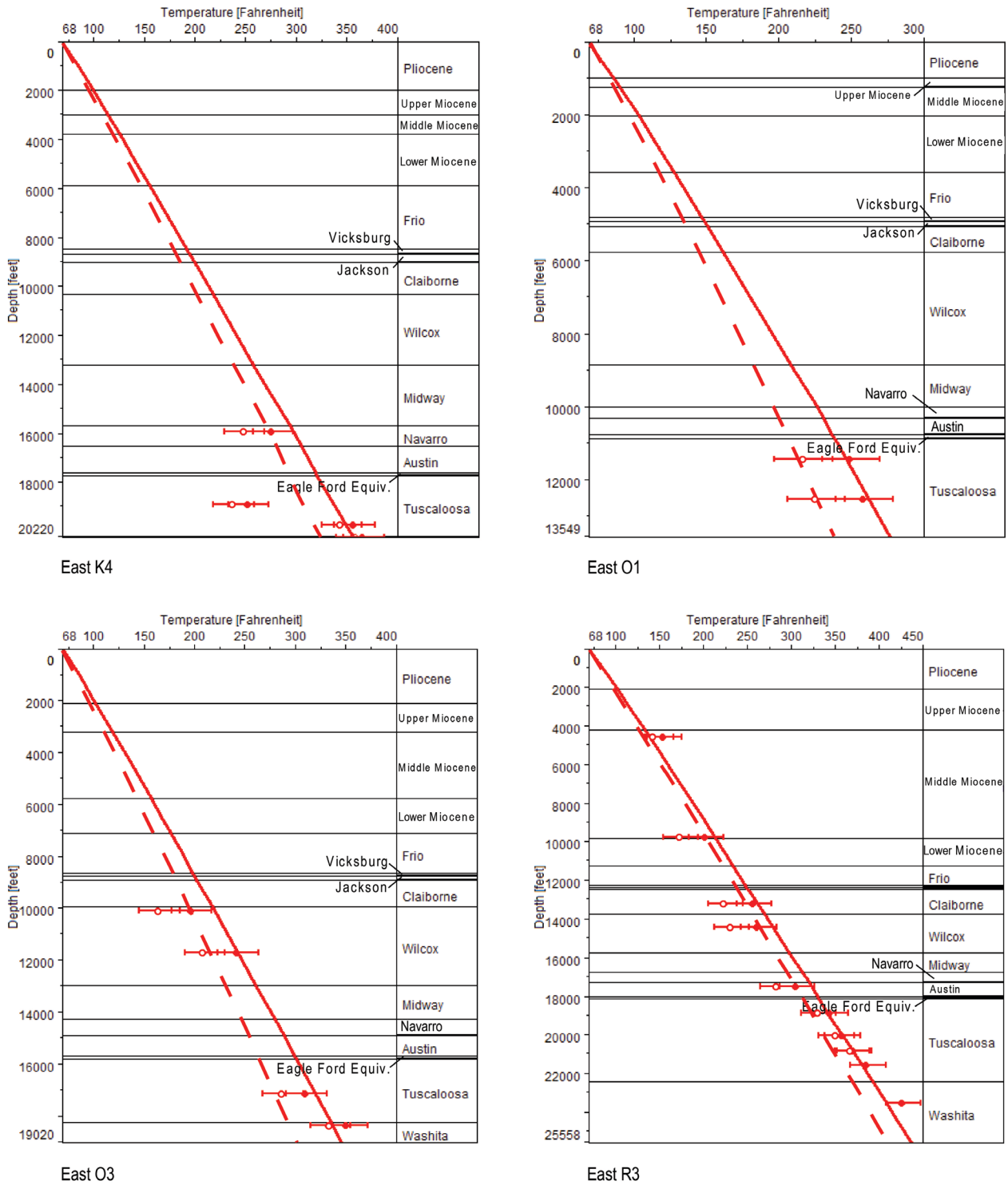

Figure 6. Calculated temperature profiles of modeled wells; see figure 2 for well locations. Dashed-line profiles based on uncorrected reservoir and bottom-hole temperatures (open circles); solid-line profiles computed from corrected bore-hole temperatures (closed circles). Error bars for temperature data are ±20°F. Corrected and uncorrected temperatures are reported on the cross sections used in the study.—Continued

The paleothermal histories at the modeled well locations were evaluated using the Easy% R_o kinetic algorithm of Sweeney and Burnham (1990). Easy%R_o, which processes multiple parallel reactions as organic matter is converted to petroleum, generates an R_o profile as a function of burial depth for each thermal-history simulation; this modeled profile can be compared with measured and computed R_o values. In the present study, R_o data for the Wilcox Formation were limited to the two wells (North-I9 and West-H4) having measured values (one value per well) (Peter Warwick, USGS, written commun., 2007). However, R_o data for the Wilcox were available for paleothermal analysis from some wells in Louisiana other than those used in the present study and also from wells in Texas (McDade and others, 1993; McDade, 2002; Paul Lillis, written commun., 2006). Two R_o-depth curves, one based on Louisiana R_o values and the other computed from Texas R_o values (Elisabeth Rowan, written commun., 2007) are shown in figure 7. It is noteworthy that the curves have the same surface intercepts (≈0.28 percent R_o) but different maturation gradients—Louisiana, 0.02 percent R_o /1,000 ft; Texas, 0.05 percent Ro/1,000 ft. The difference in R_o gradients is interpreted to reflect regional variations in paleoheat flow. To evaluate the paleothermal regime at each well locality, two R_o profiles (referred to as scenarios 1 and 2) were generated for each well, one (scenario 1) utilizing uncorrected reservoir temperatures and the other (scenario 2) utilizing corrected reservoir temperatures (fig. 8). In the model simulations, both scenarios assume constant paleothermal conditions through time, an assumption that is considered reasonable inasmuch as the burial and thermal history of the Gulf Coast has not changed during the last 60 to 75 million years (m.y.) (Driskill and others, 1988). In the majority of wells, R_o profiles based on scenario 1 plot close to or within the error limits of R_o values for the Wilcox Formation computed from the Louisiana R_o-depth curve; in contrast, profiles based on scenario 2 tend to fall within the error bars of Wilcox values for Texas.

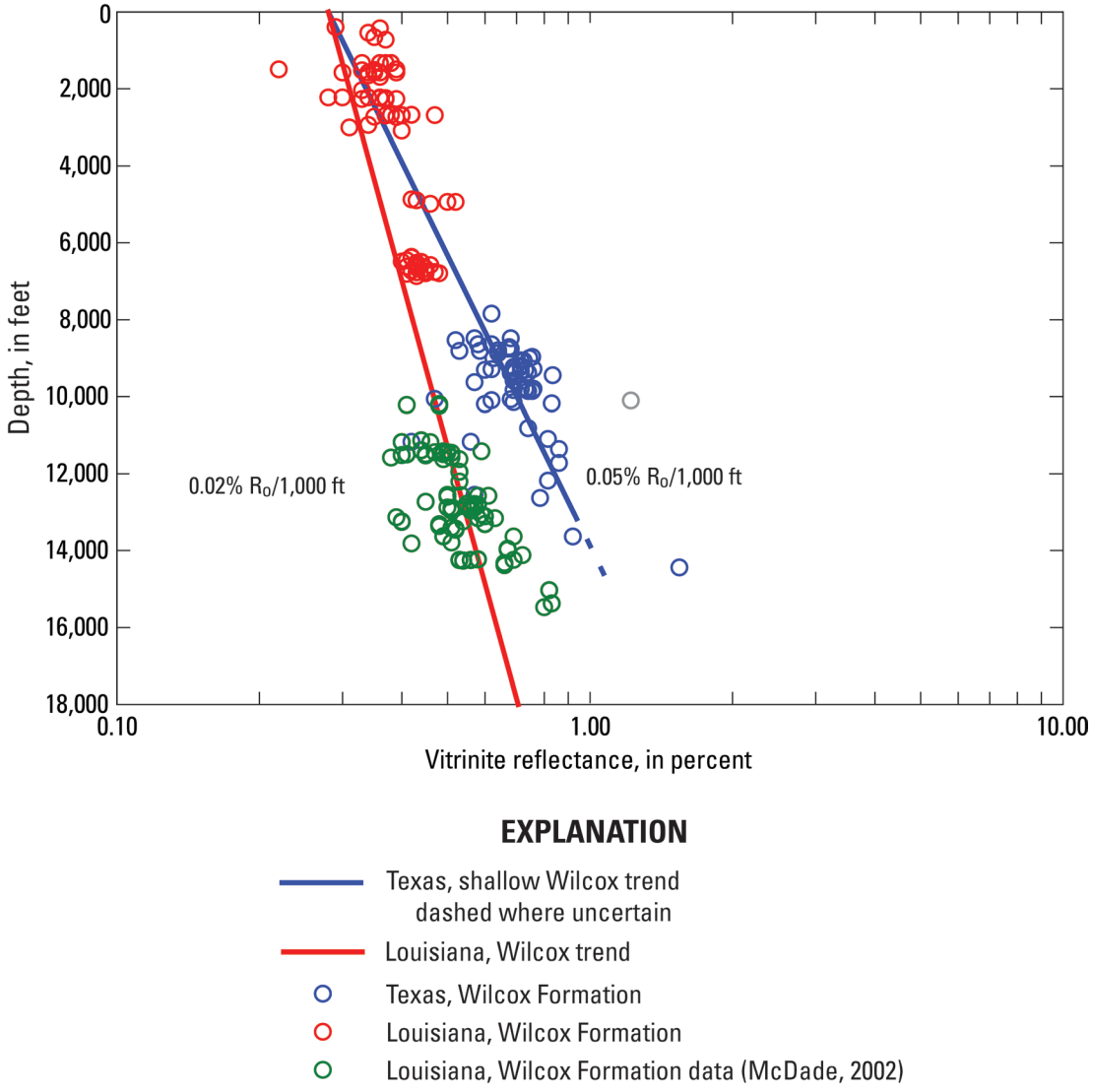

Figure 7. Vitrinite reflectance (R_o)–depth trends for measured data in the Wilcox Formation, Texas and Louisiana.

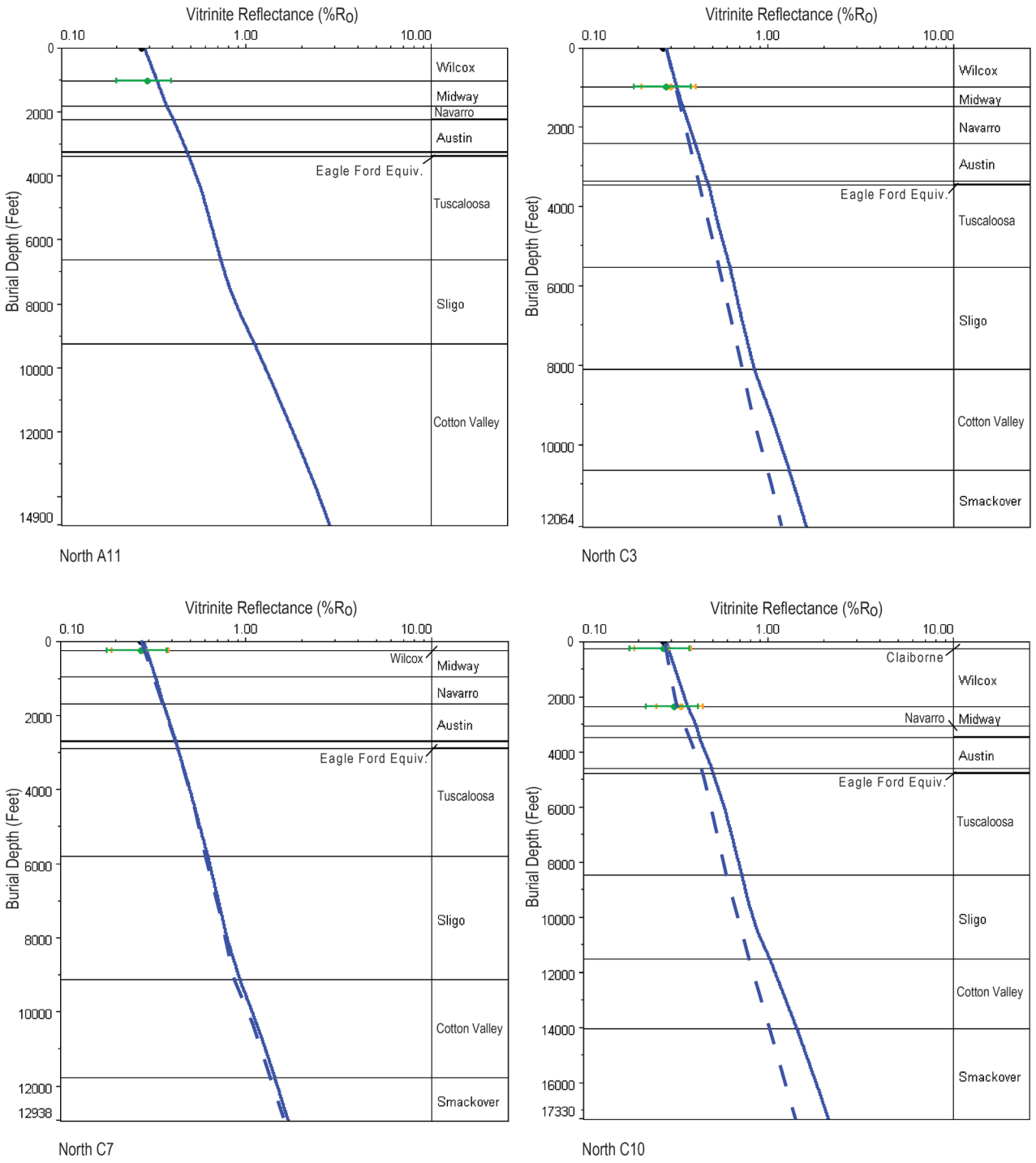

Figure 8. Calculated vitrinite reflectance (percentage R_o) profiles for modeled wells; see figure 2 for well locations. Dashed-line R_o profile utilized uncorrected borehole temperatures in the calculation and the solid-line profile used corrected temperatures in the calculation. R_o values for the top and base of the Wilcox computed from the R_o-depth trend in Louisiana (green circles) and Texas (yellow circles) (see fig. 7) are shown for comparison. Pink circles (wells North I9 and West H4) represent measured R_o values (Peter Warwick, USGS, written commun., 2007). Error bars for measured and computed values are ± 0.2 percent R_o.

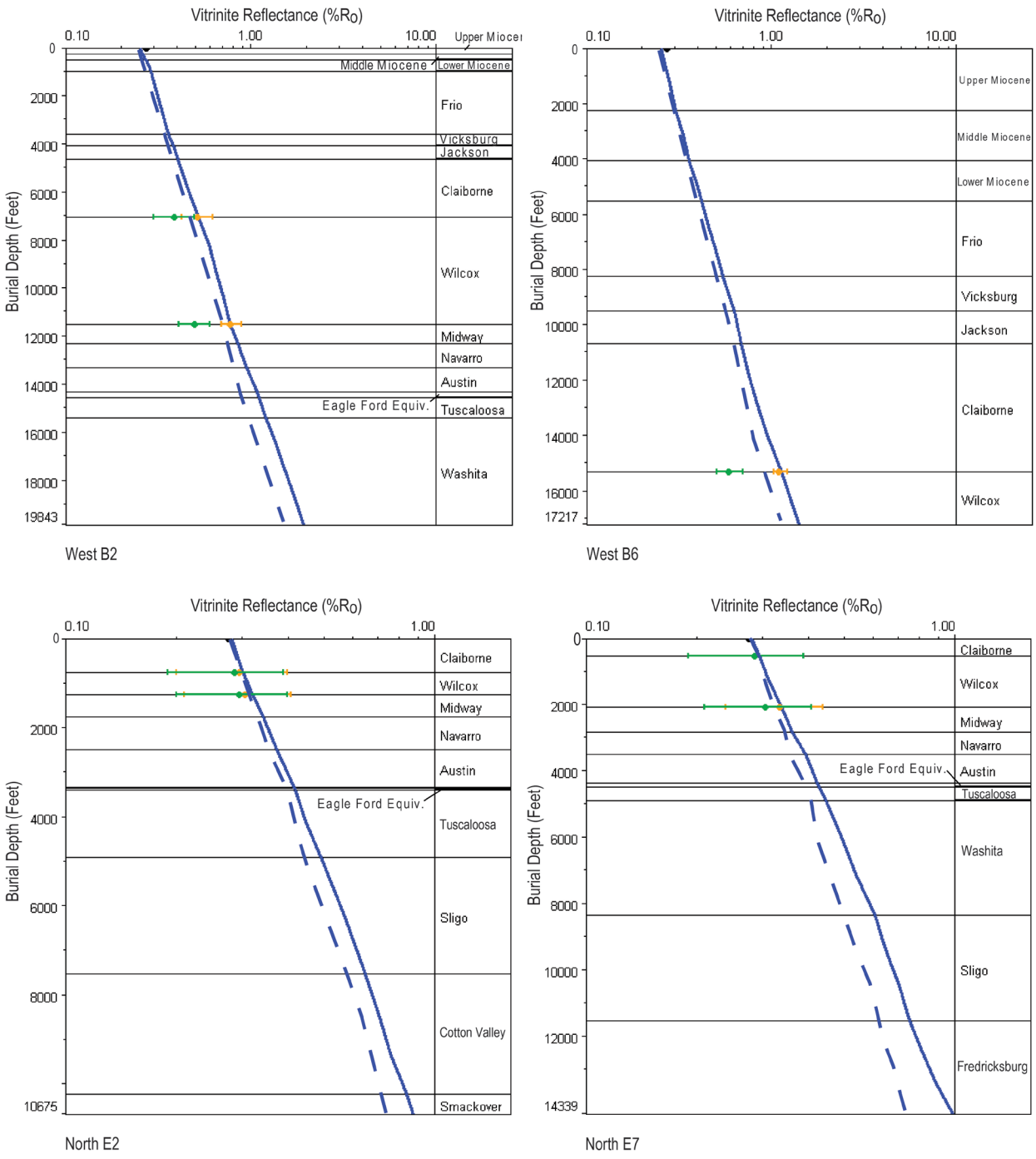

Figure 8. Calculated vitrinite reflectance (percentage R_o) profiles for modeled wells; see figure 2 for well locations. Dashed-line R_o profile utilized uncorrected borehole temperatures in the calculation and the solid-line profile used corrected temperatures in the calculation. R_o values for the top and base of the Wilcox computed from the R_o -depth trend in Louisiana (green circles) and Texas (yellow circles) (see fig. 7) are shown for comparison. Pink circles (wells North I9 and West H4) represent measured R_o values (Peter Warwick, USGS, written commun., 2007). Error bars for measured and computed values are ± 0.2 percent R_o.—Continued

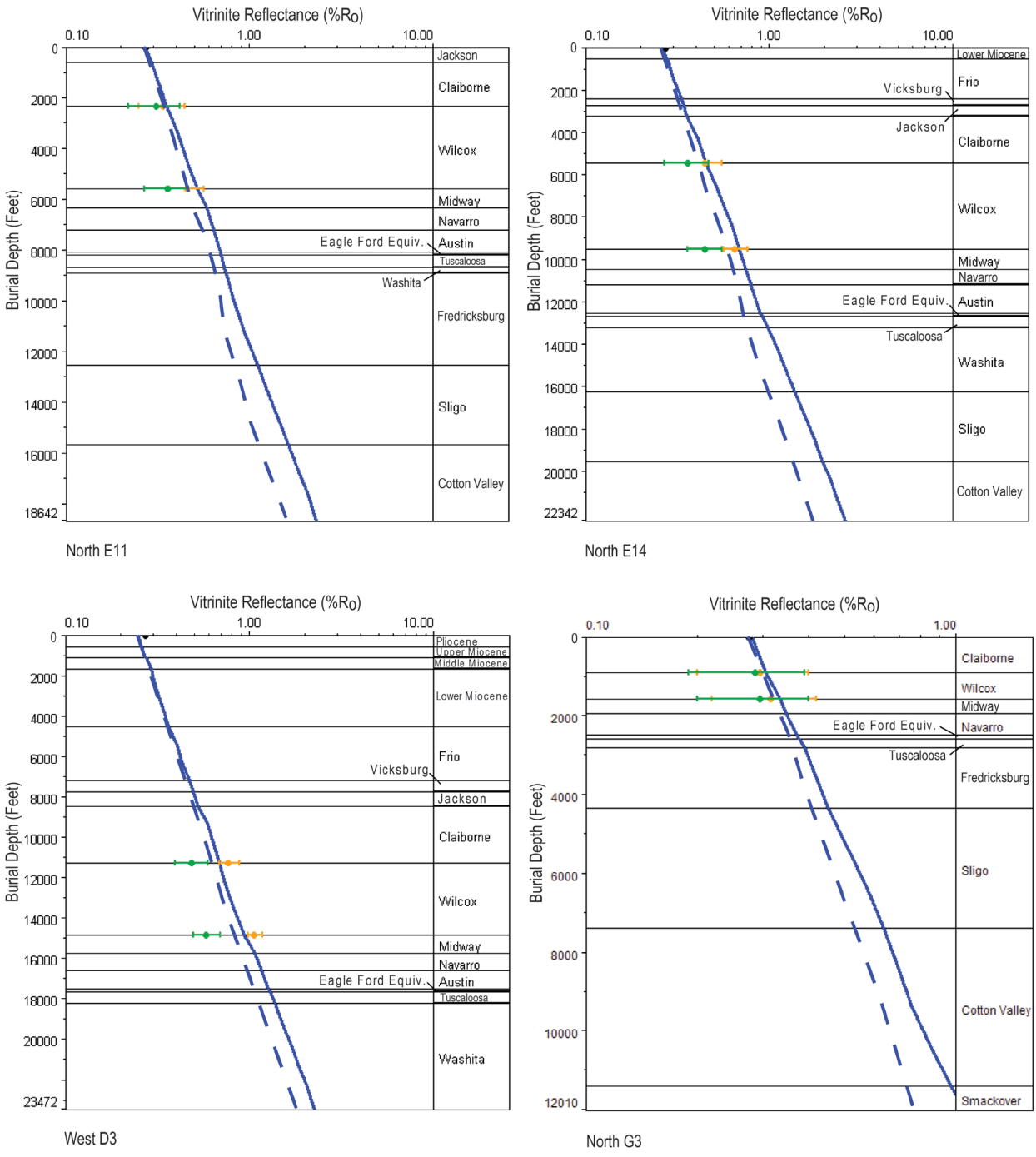

Figure 8. Calculated vitrinite reflectance (percentage R_o) profiles for modeled wells; see figure 2 for well locations. Dashed-line R_o profile utilized uncorrected borehole temperatures in the calculation and the solid-line profile used corrected temperatures in the calculation. R_o values for the top and base of the Wilcox computed from the R_o -depth trend in Louisiana (green circles) and Texas (yellow circles) (see fig. 7) are shown for comparison. Pink circles (wells North I9 and West H4) represent measured R_o values (Peter Warwick, USGS, written commun., 2007). Error bars for measured and computed values are ± 0.2 percent R_o.—Continued

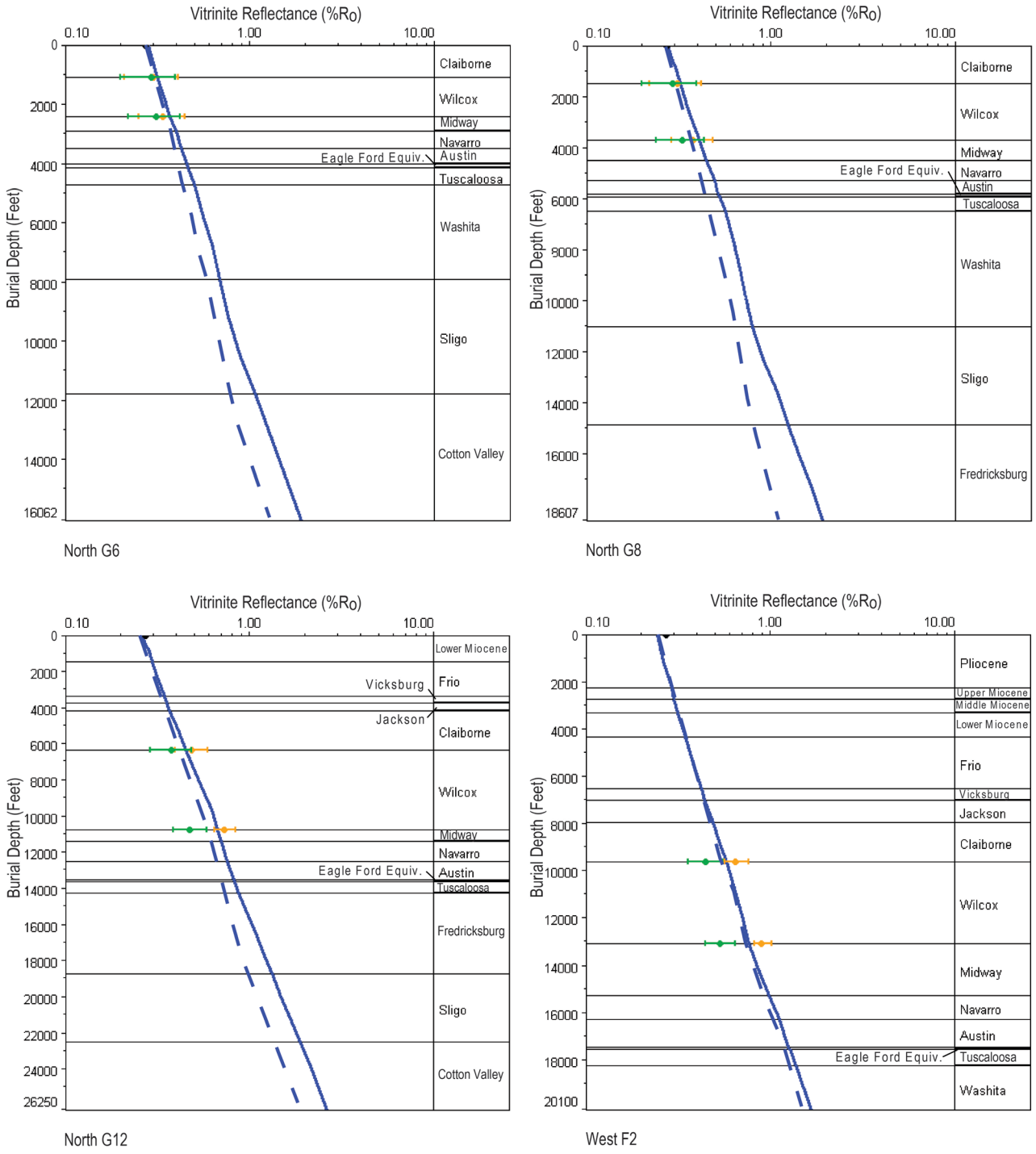

Figure 8. Calculated vitrinite reflectance (percentage R_o) profiles for modeled wells; see figure 2 for well locations. Dashed-line R_o profile utilized uncorrected borehole temperatures in the calculation and the solid-line profile used corrected temperatures in the calculation. R_o values for the top and base of the Wilcox computed from the R_o -depth trend in Louisiana (green circles) and Texas (yellow circles) (see fig. 7) are shown for comparison. Pink circles (wells North I9 and West H4) represent measured R_o values (Peter Warwick, USGS, written commun., 2007). Error bars for measured and computed values are ± 0.2 percent R_o.—Continued

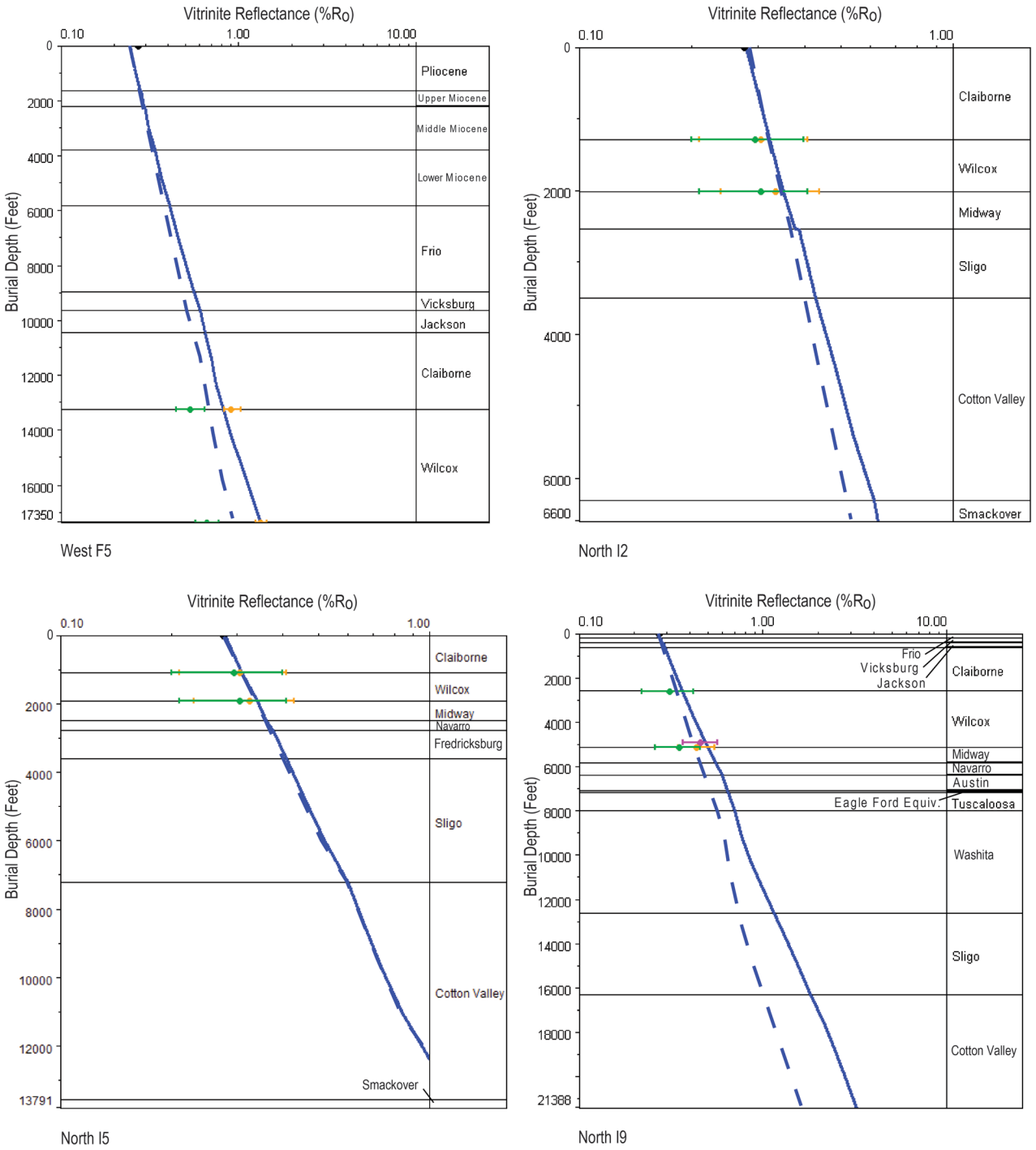

Figure 8. Calculated vitrinite reflectance (percentage R_o) profiles for modeled wells; see figure 2 for well locations. Dashed-line R_o profile utilized uncorrected borehole temperatures in the calculation and the solid-line profile used corrected temperatures in the calculation. R_o values for the top and base of the Wilcox computed from the R_o -depth trend in Louisiana (green circles) and Texas (yellow circles) (see fig. 7) are shown for comparison. Pink circles (wells North I9 and West H4) represent measured R_o values (Peter Warwick, USGS, written commun., 2007). Error bars for measured and computed values are ± 0.2 percent R_o.—Continued

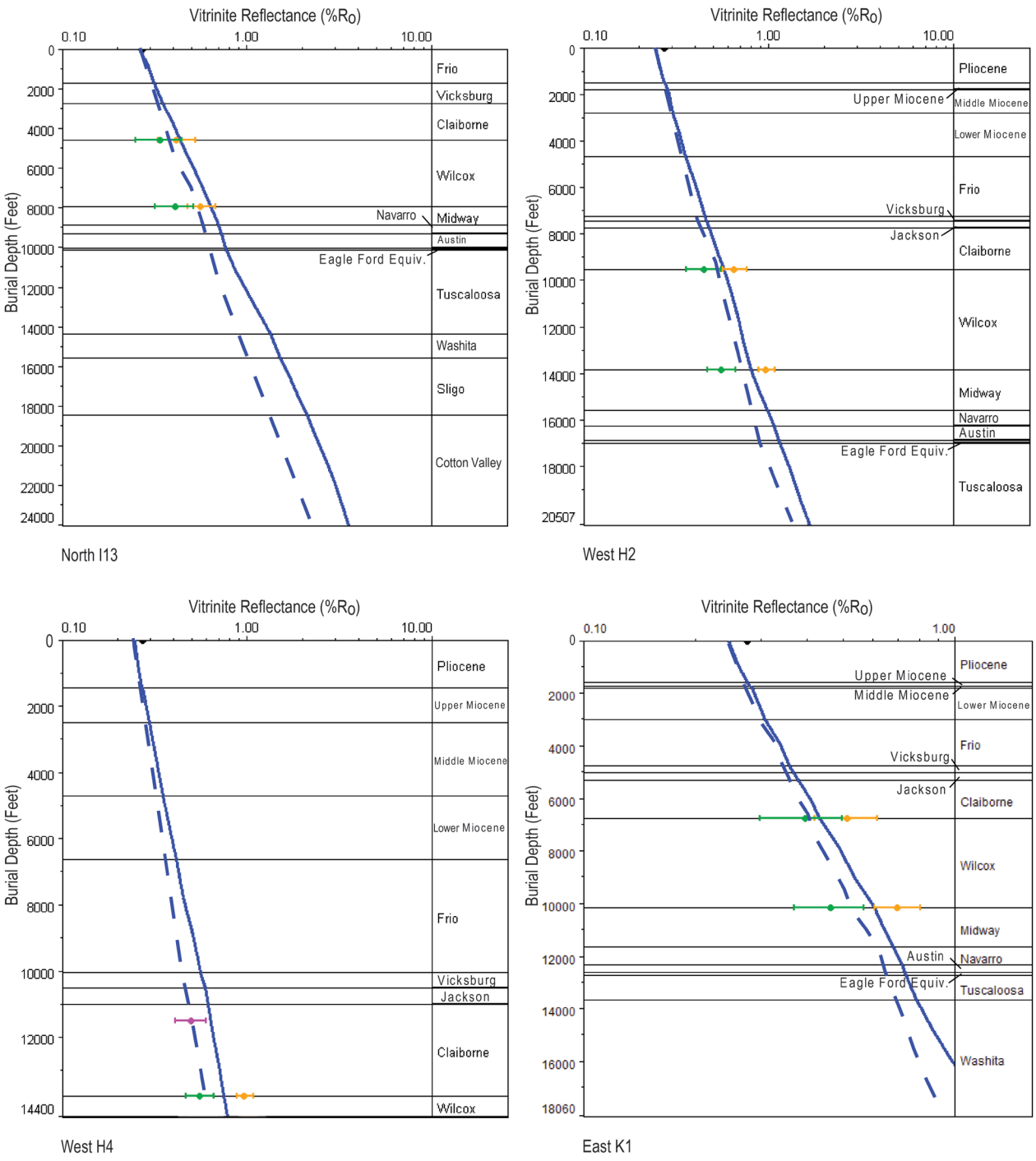

Figure 8. Calculated vitrinite reflectance (percentage R_o) profiles for modeled wells; see figure 2 for well locations. Dashed-line R_o profile utilized uncorrected borehole temperatures in the calculation and the solid-line profile used corrected temperatures in the calculation. R_o values for the top and base of the Wilcox computed from the R_o -depth trend in Louisiana (green circles) and Texas (yellow circles) (see fig. 7) are shown for comparison. Pink circles (wells North I9 and West H4) represent measured R_o values (Peter Warwick, USGS, written commun., 2007). Error bars for measured and computed values are ± 0.2 percent R_o.—Continued

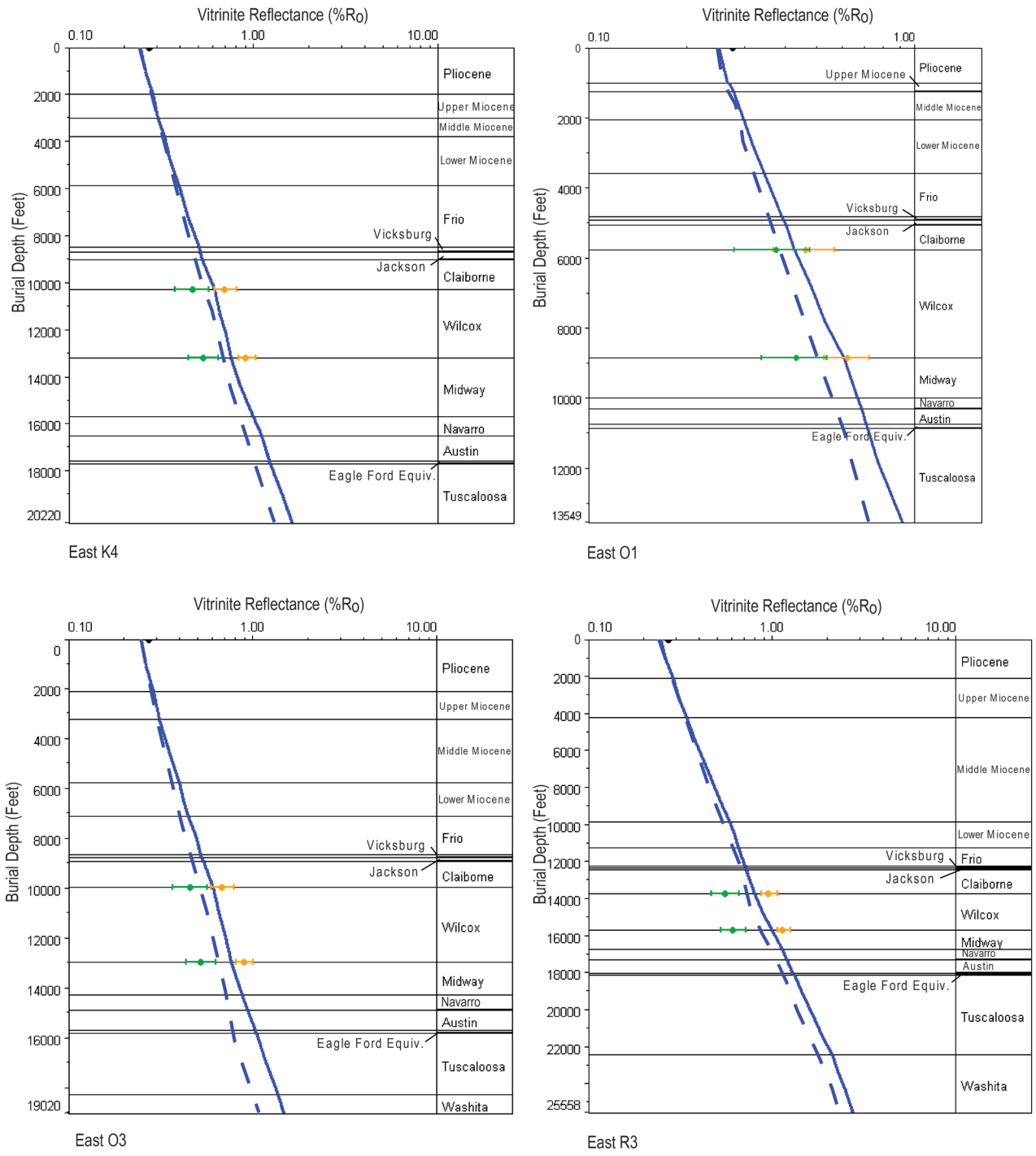

Figure 8. Calculated vitrinite reflectance (percentage R_o) profiles for modeled wells; see figure 2 for well locations. Dashed-line R_o profile utilized uncorrected borehole temperatures in the calculation and the solid-line profile used corrected temperatures in the calculation. R_o values for the top and base of the Wilcox computed from the R_o -depth trend in Louisiana (green circles) and Texas (yellow circles) (see fig. 7) are shown for comparison. Pink circles (wells North I9 and West H4) represent measured R_o values (Peter Warwick, USGS, written commun., 2007). Error bars for measured and computed values are ± 0.2 percent R_o.—Continued

Causes for the discrepancy between the computed R_o curves and modeled profiles are speculative. Generally, bottom-hole and reservoir-temperature data corrected for drilling-circulation times are considered a reasonable representation of the present subsurface thermal conditions of an area. The fact that scenario 2, which utilized corrected reservoir temperatures, overestimates R_o relative to the Louisiana R_o-depth trend indicates that the correction factor applied to the initial temperature measurements might be invalid. Another possibility is that the vitrinite reflectance measurements performed on samples of shale, as reported by McDade and others (1993) (see fig. 7), are low compared to measurements on coals, which are considered more reliable. Coals compose the bulk of the samples analyzed in Texas, whereas shales were mainly analyzed in Louisiana. A comparison of R_o and temperature of maximum hydrocarbon generation (Tmax) data for the same samples in the McDade data set (McDade and others, 1993) shows good correlation, indicating that the shale samples were not affected by vitrinite suppression. Further analysis is required to fully evaluate the measured R_o data reported for the Wilcox Formation.

Wilcox Formation Burial Temperatures and Petroleum Generation History

The temperatures and timing of petroleum generation were determined for the Wilcox Formation using scenario 2. Because the Wilcox source facies may be oil prone or gas prone, generation models were simulated for both oil (fig. 9, table 2) and gas (fig. 10, table 3). The models in figures 9 and 10 are referred to as either updip (north) or downdip (south) of the Lower Cretaceous shelf edge. The Cretaceous shelf edge (fig. 2) coincides with the updip limit of terrestrial-type oil that originated in Tertiary rocks, as depicted by Hood and others (2002), and it is useful for purposes of discussion. Tables 2 and 3 list depths of burial and temperatures for specific petroleum generation events reported by geologic age.

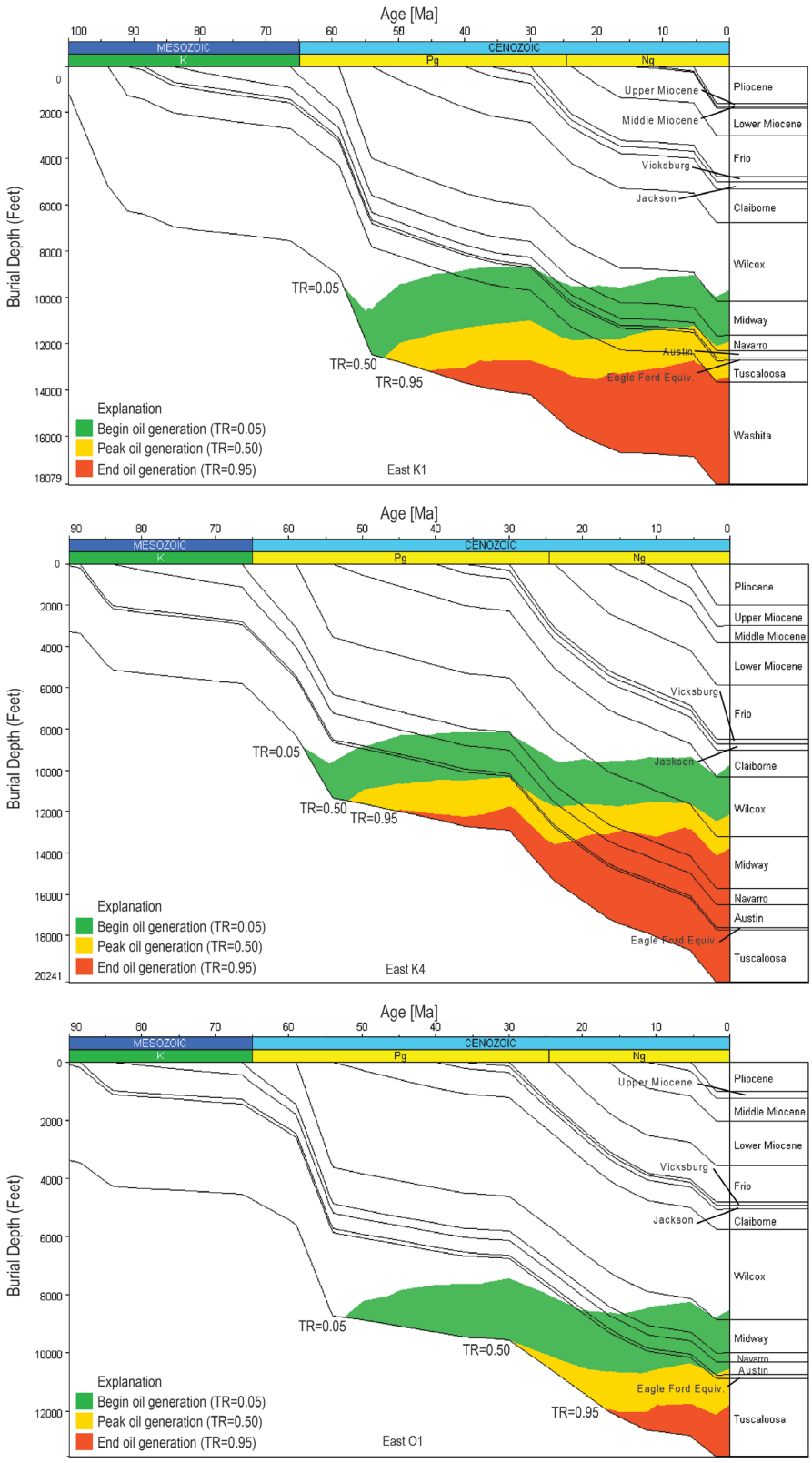

Figure 9. Burial-history curves showing timing of oil generation in the Wilcox Formation based on transformation ratios (TR). See figure 2 for well locations. Ma, mega-annum.

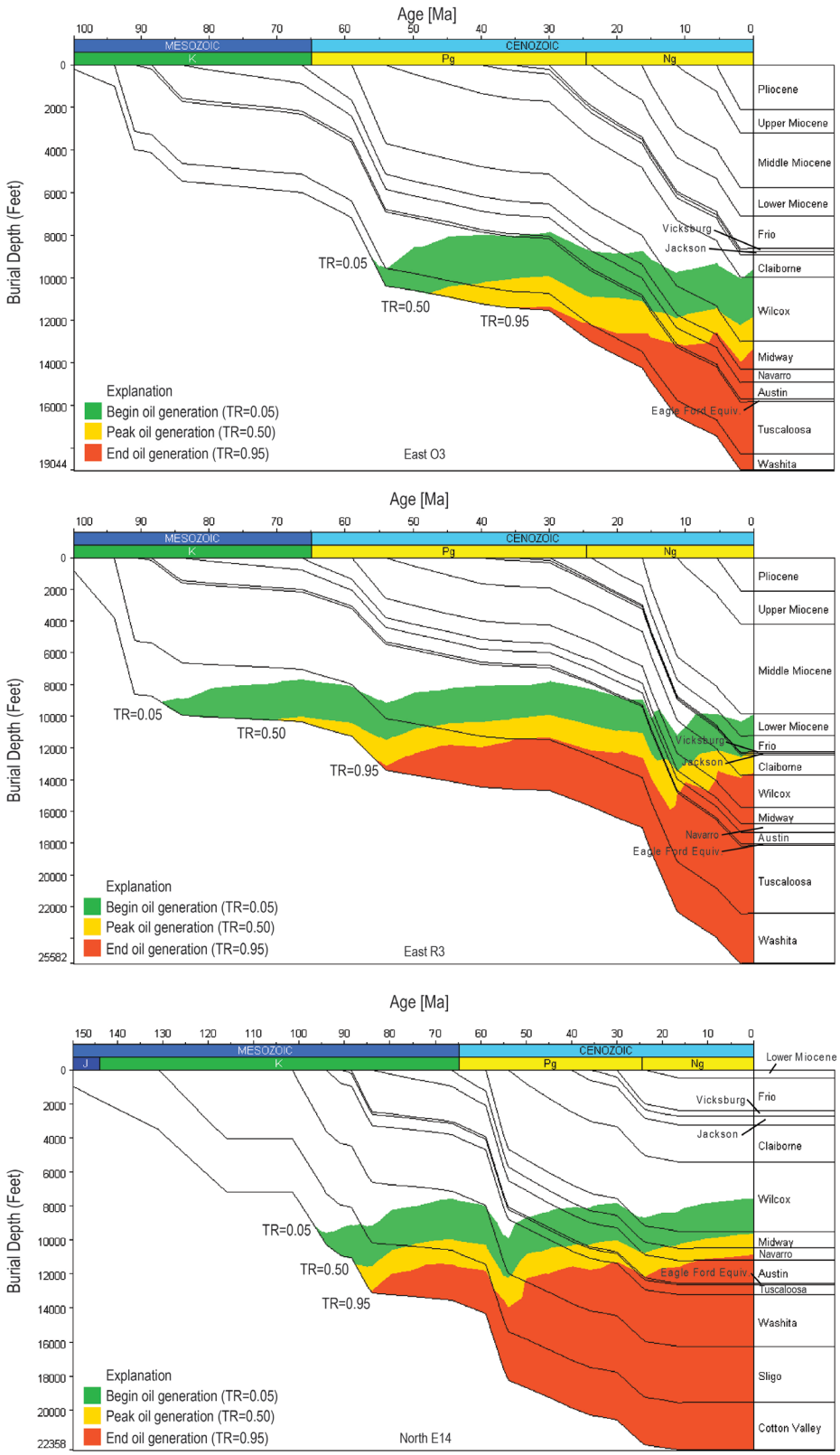

Figure 9. Burial-history curves showing timing of oil generation in the Wilcox Formation based on transformation ratios (TR). See figure 2 for well locations. Ma, mega-annum.—Continued

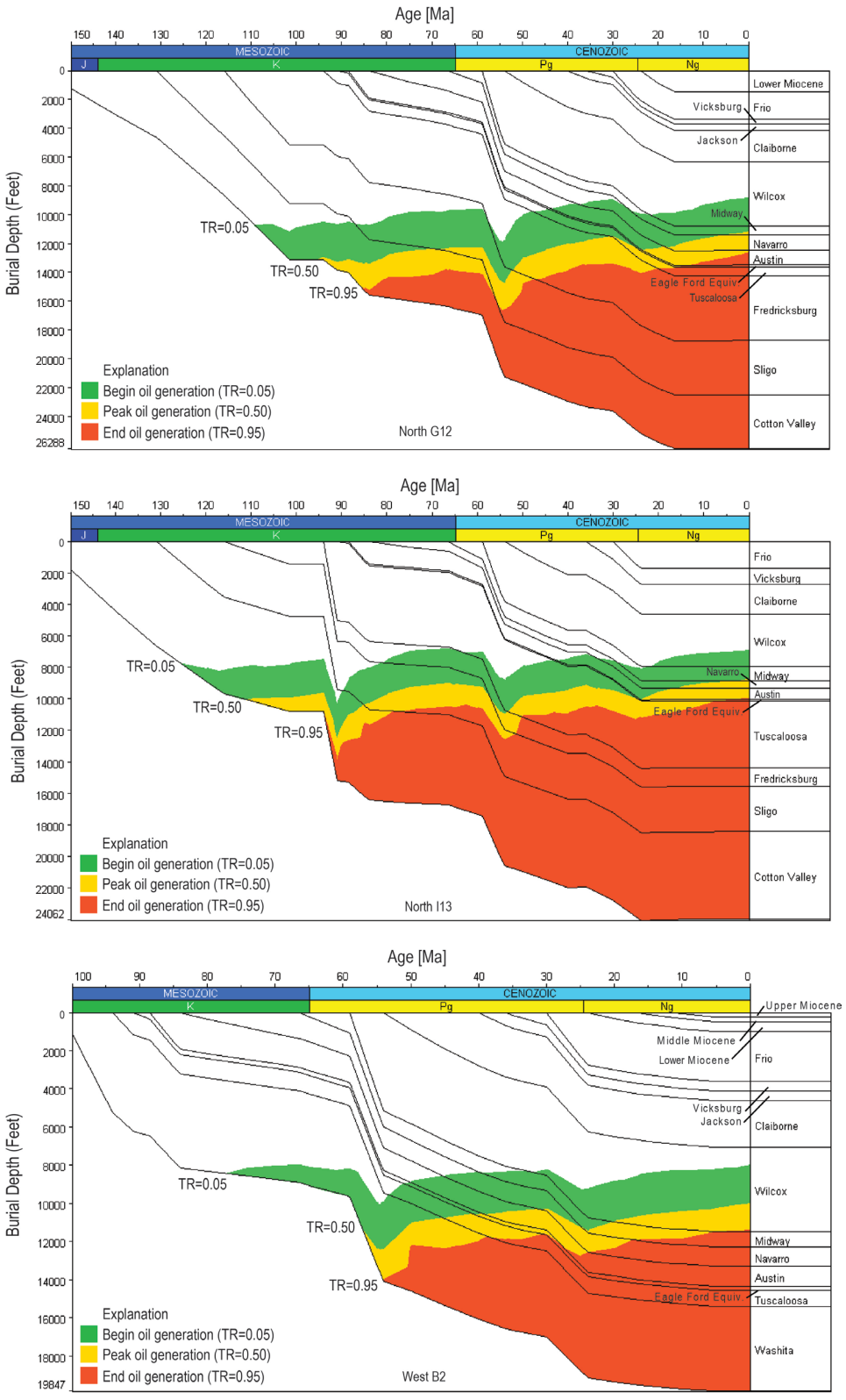

Figure 9. Burial-history curves showing timing of oil generation in the Wilcox Formation based on transformation ratios (TR). See figure 2 for well locations. Ma, mega-annum.—Continued

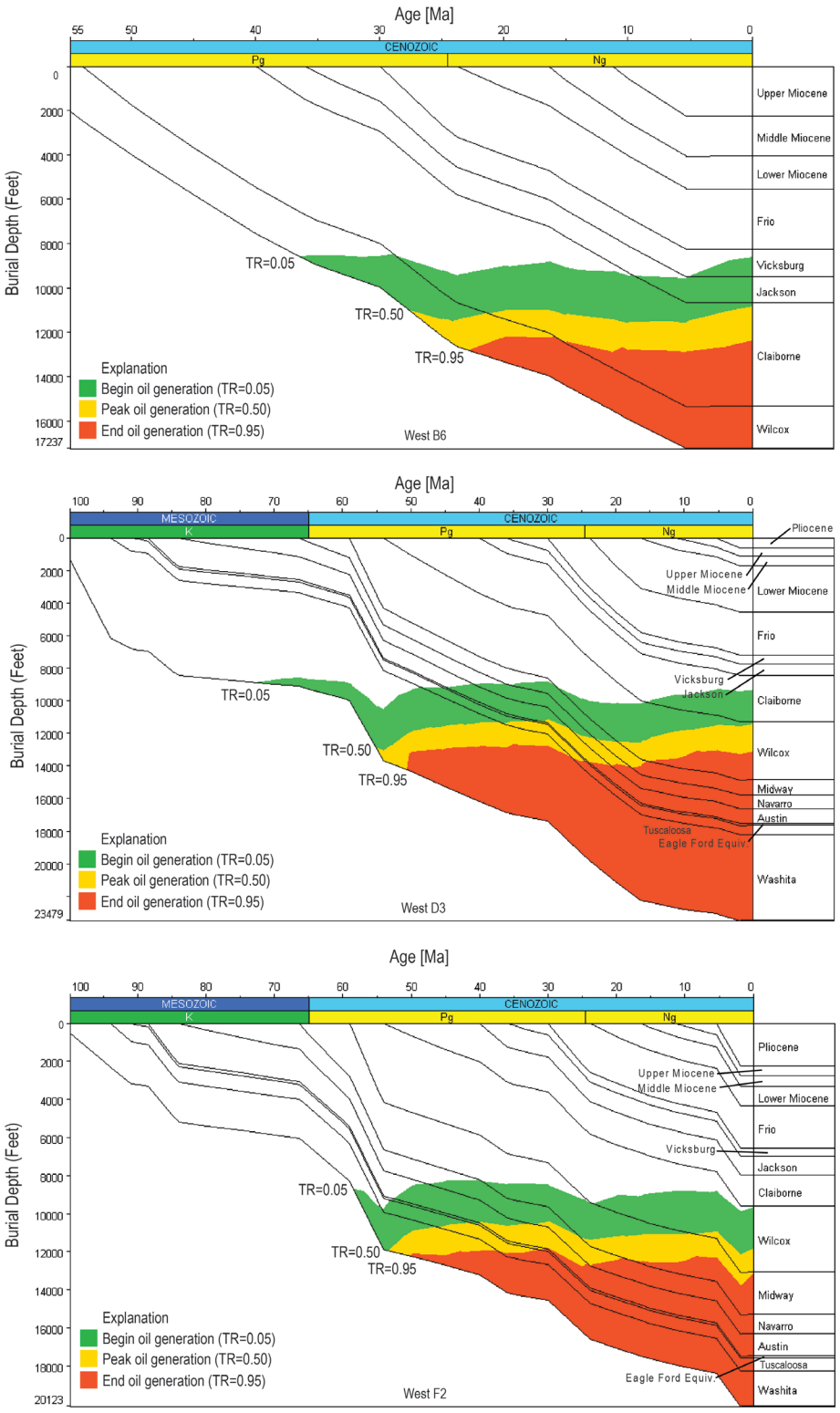

Figure 9. Burial-history curves showing timing of oil generation in the Wilcox Formation based on transformation ratios (TR). See figure 2 for well locations. Ma, mega-annum.—Continued

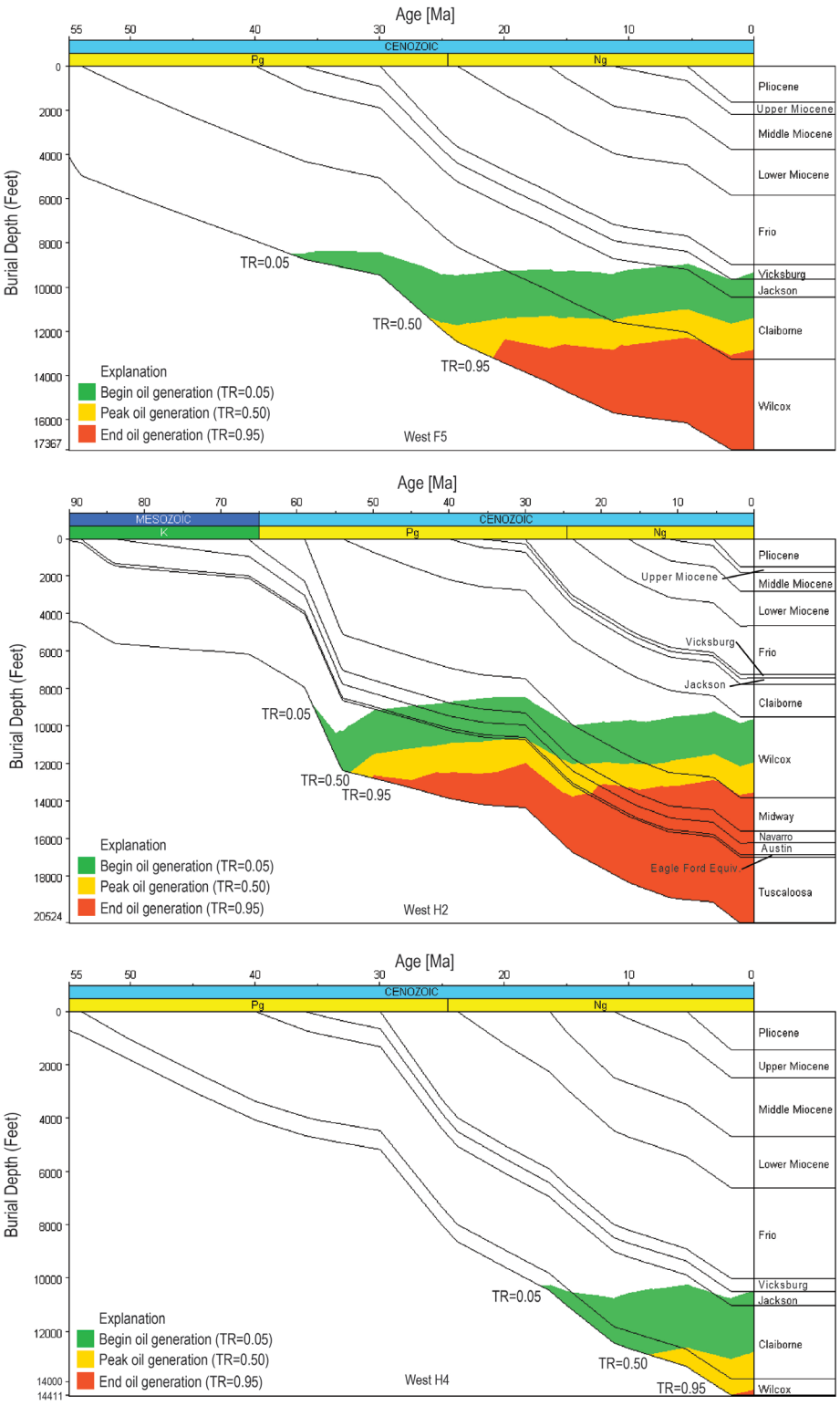

Figure 9. Burial-history curves showing timing of oil generation in the Wilcox Formation based on transformation ratios (TR). See figure 2 for well locations. Ma, mega-annum.—Continued

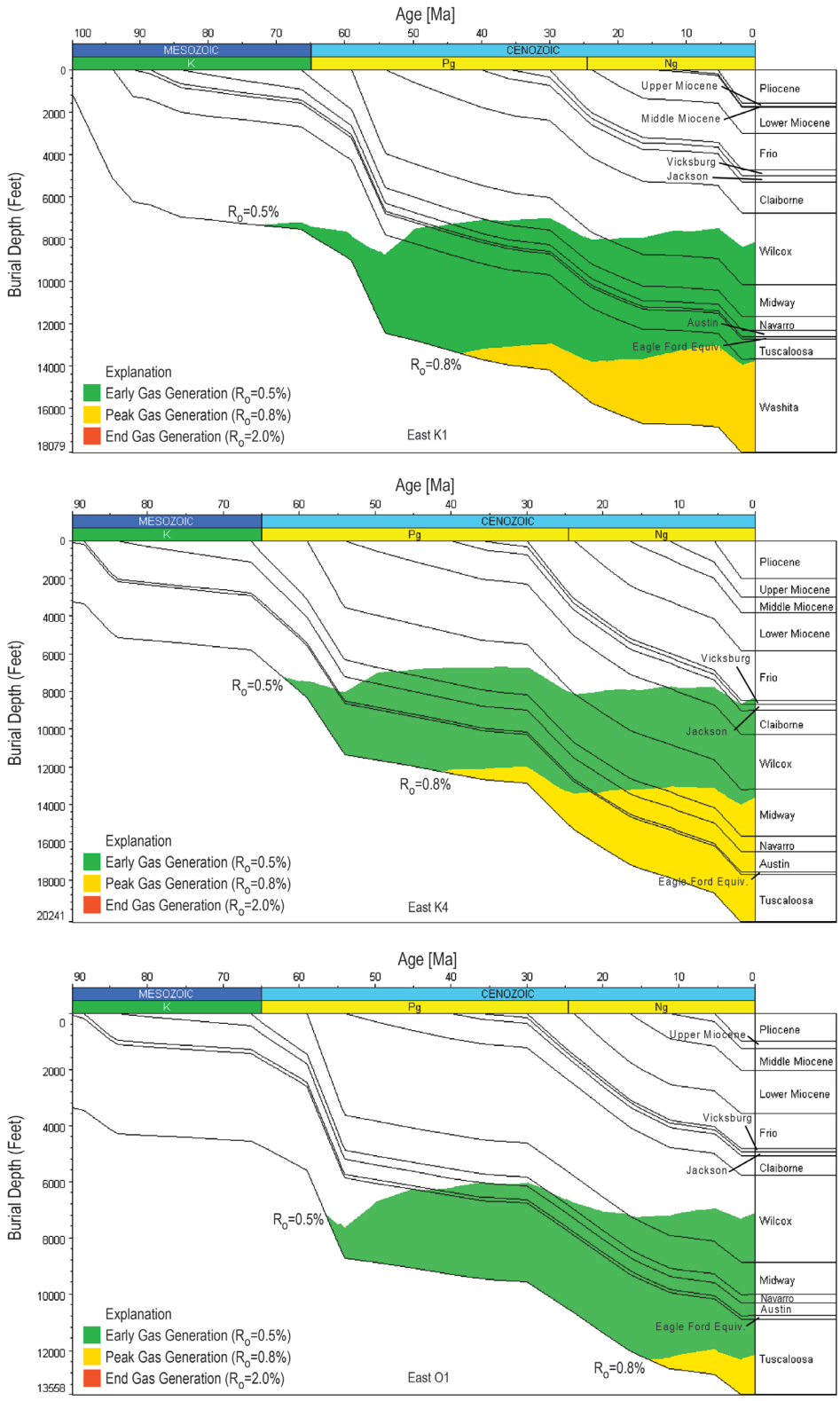

Figure 10. Burial-history curves showing timing of gas generation in the Wilcox Formation based on vitrinite reflectance (R_o). See figure 2 for well locations. Ma, mega-annum.

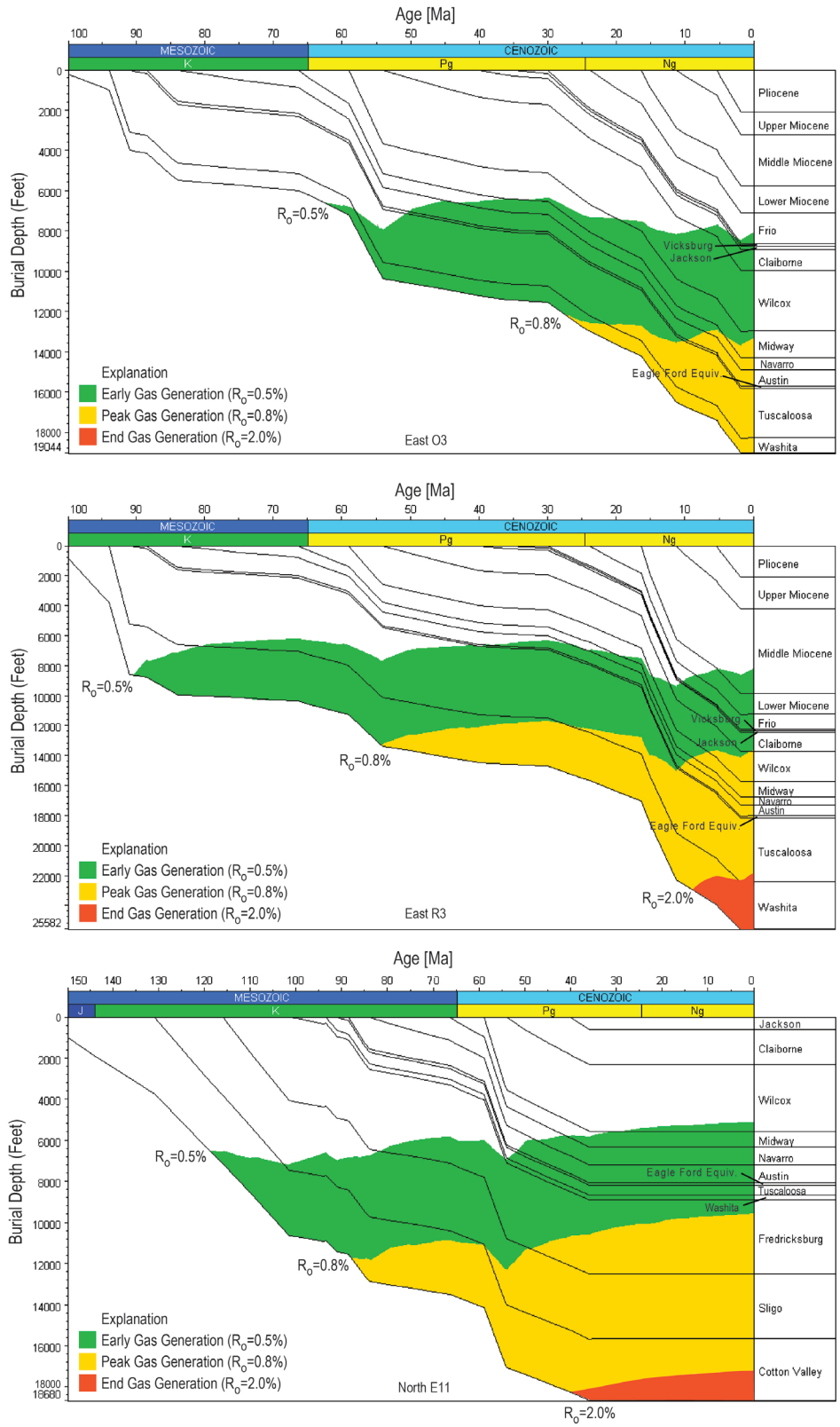

Figure 10. Burial-history curves showing timing of gas generation in the Wilcox Formation based on vitrinite reflectance (R_o). See figure 2 for well locations. Ma, mega-annum.—Continued

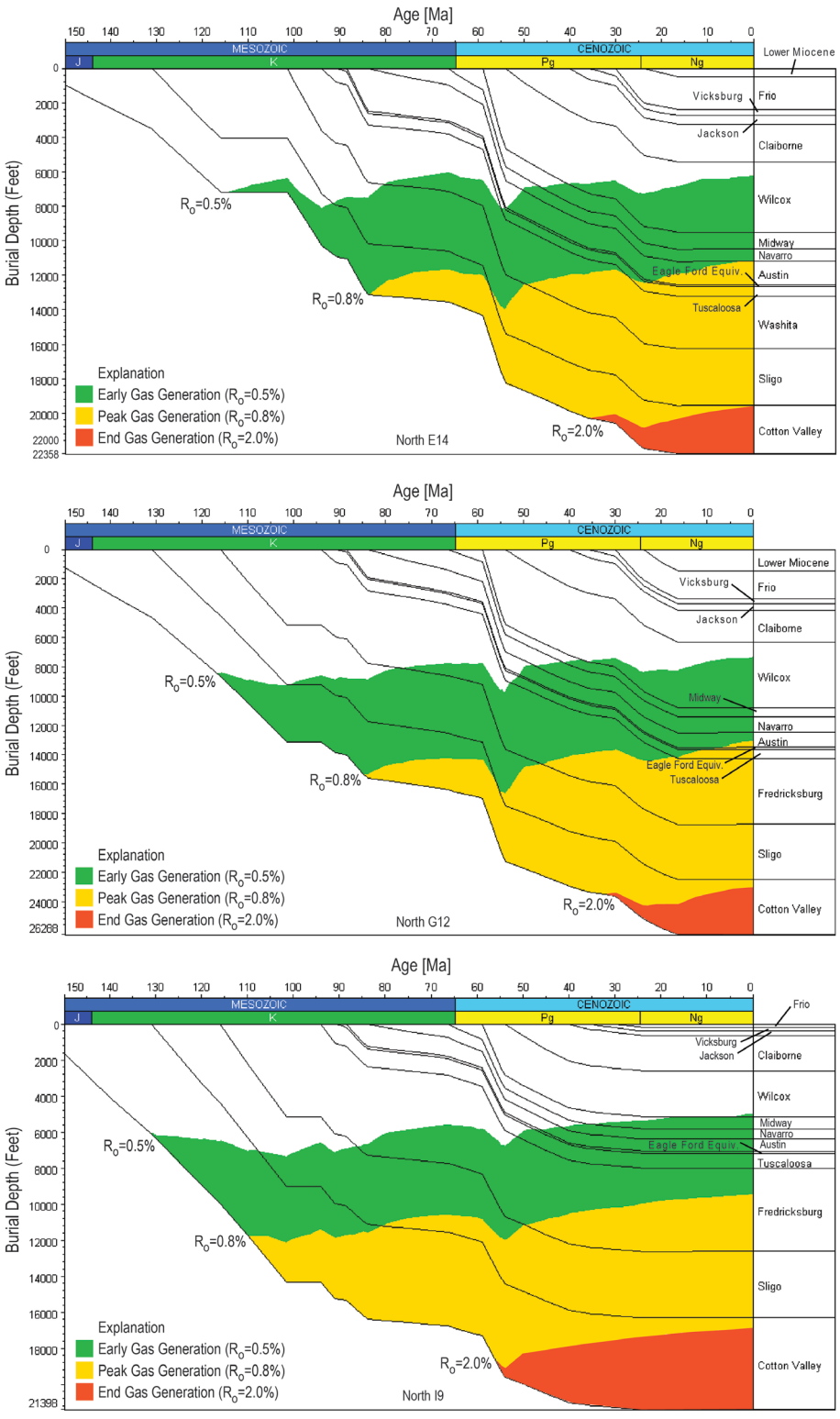

Figure 10. Burial-history curves showing timing of gas generation in the Wilcox Formation based on vitrinite reflectance (R_o). See figure 2 for well locations. Ma, mega-annum.—Continued

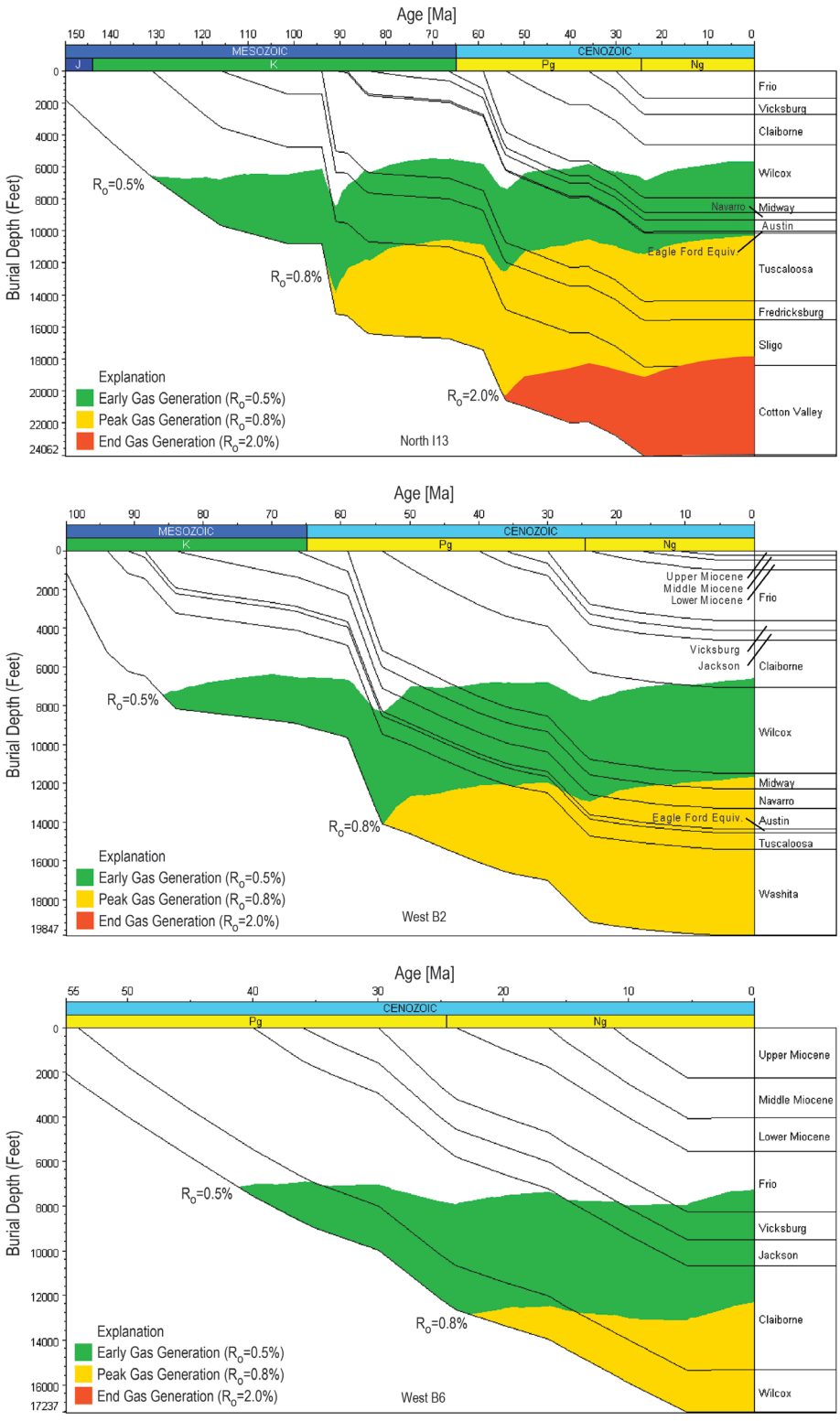

Figure 10. Burial-history curves showing timing of gas generation in the Wilcox Formation based on vitrinite reflectance (R_o). See figure 2 for well locations. Ma, mega-annum.—Continued

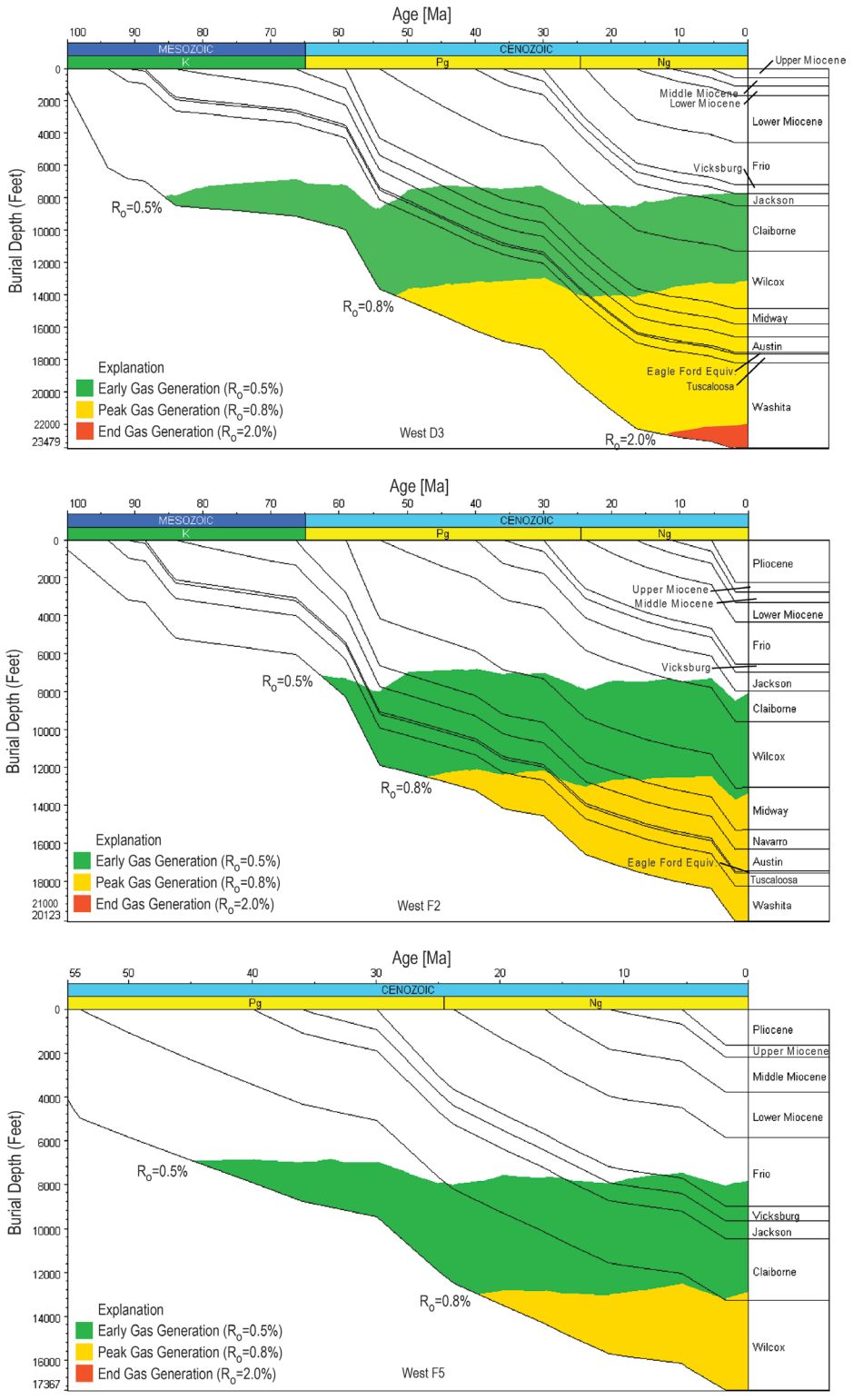

Figure 10. Burial-history curves showing timing of gas generation in the Wilcox Formation based on vitrinite reflectance (R_o). See figure 2 for well locations. Ma, mega-annum.—Continued

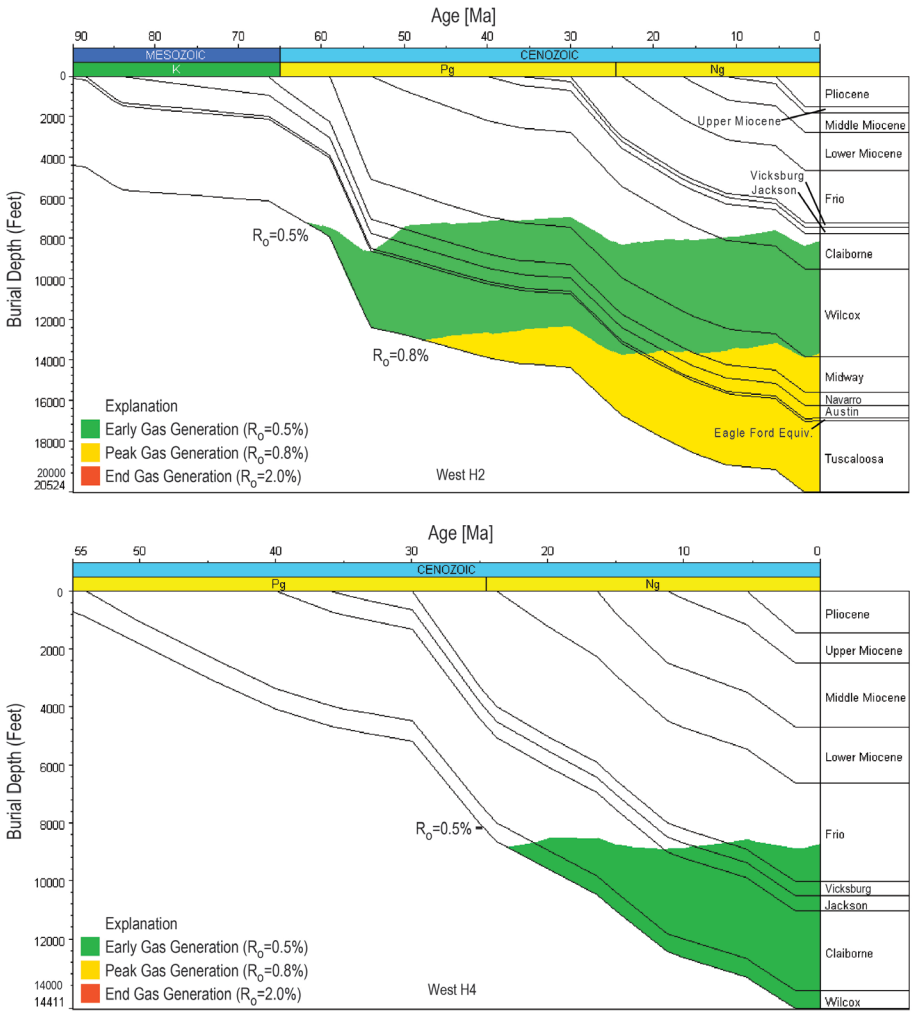

Figure 10. Burial-history curves showing timing of gas generation in the Wilcox Formation based on vitrinite reflectance (R_o). See figure 2 for well locations. Ma, mega-annum.—Continued

Table 2. Three transformation ratios compared with age, depth, and temperature of oil generation in the Wilcox Formation in modeled Louisiana wells).

[TR, transformation ratio—shown at top of Wilcox (*A*) and base of Wilcox (*B*); Ma, mega-annum; ft, foot; Temp. (F), temperature, degrees Fahrenheit; NG, no generation]

A.

Well	Top of Wilcox Formation, Louisiana								
	Start oil generation (TR = 0.05)			Peak oil generation (TR = 0.50)			End oil generation (TR = 0.95)		
	Age (Ma)	Depth (ft)	Temp. (F)	Age (Ma)	Depth (ft)	Temp. (F)	Age (Ma)	Depth (ft)	Temp. (F)
North A11	NG	NG	NG	NG	NG	NG	NG	NG	NG
North C3	NG	NG	NG	NG	NG	NG	NG	NG	NG
North C7	NG	NG	NG	NG	NG	NG	NG	NG	NG
North C10	NG	NG	NG	NG	NG	NG	NG	NG	NG
West B2	NG	NG	NG	NG	NG	NG	NG	NG	NG
West B6	29	8,468	207	22	11,102	244	16	12,194	258
North E2	NG	NG	NG	NG	NG	NG	NG	NG	NG
North E7	NG	NG	NG	NG	NG	NG	NG	NG	NG
North E11	NG	NG	NG	NG	NG	NG	NG	NG	NG
North E14	NG	NG	NG	NG	NG	NG	NG	NG	NG
West D3	16	10,048	213	0	11,278	231	NG	NG	NG
North G3	NG	NG	NG	NG	NG	NG	NG	NG	NG
North G6	NG	NG	NG	NG	NG	NG	NG	NG	NG
North G8	NG	NG	NG	NG	NG	NG	NG	NG	NG
North G12	NG	NG	NG	NG	NG	NG	NG	NG	NG
West F2	0	9,622	209	NG	NG	NG	NG	NG	NG
West F5	20	9,214	213	12	11,451	243	4	12,361	255
North I2	NG	NG	NG	NG	NG	NG	NG	NG	NG
North I5	NG	NG	NG	NG	NG	NG	NG	NG	NG
North I9	NG	NG	NG	NG	NG	NG	NG	NG	NG
North I13	NG	NG	NG	NG	NG	NG	NG	NG	NG
West H2	0	9,590	204	NG	NG	NG	NG	NG	NG
West H4	15	10,478	212	6	12,649	239	NG	NG	NG
East K1	NG	NG	NG	NG	NG	NG	NG	NG	NG
East K4	2	10,209	213	NG	NG	NG	NG	NG	NG
East O1	NG	NG	NG	NG	NG	NG	NG	NG	NG
East O3	2	9,896	213	NG	NG	NG	NG	NG	NG
East R3	10	10,668	222	5	12,121	246	2	13,685	265

Table 2. Three transformation ratios compared with age, depth, and temperature of oil generation in the Wilcox Formation in modeled Louisiana wells).—Continued

[TR, transformation ratio—shown at top of Wilcox (*A*) and base of Wilcox (*B*); Ma, mega-annum; ft, foot; Temp. (F), temperature, degrees Fahrenheit; NG, no generation]

B.

Well	Base of Wilcox Formation, Louisiana								
	Start oil generation (TR = 0.05)			Peak oil generation (TR = 0.50)			End oil generation (TR = 0.95)		
	Age (Ma)	Depth (ft)	Temp. (F)	Age (Ma)	Depth (ft)	Temp. (F)	Age (Ma)	Depth (ft)	Temp. (F)
North A11	NG	NG	NG	NG	NG	NG	NG	NG	NG
North C3	NG	NG	NG	NG	NG	NG	NG	NG	NG
North C7	NG	NG	NG	NG	NG	NG	NG	NG	NG
North C10	NG	NG	NG	NG	NG	NG	NG	NG	NG
West B2	33	8,341	205	20	10,985	240	6	11,506	245
West B6	36	8,602	210	27	11,222	245	23	12,880	267
North E2	NG	NG	NG	NG	NG	NG	NG	NG	NG
North E7	NG	NG	NG	NG	NG	NG	NG	NG	NG
North E11	NG	NG	NG	NG	NG	NG	NG	NG	NG
North E14	26	8,557	208	NG	NG	NG	NG	NG	NG
West D3	29	9,030	203	20	12,510	247	16	13,655	262
North G3	NG	NG	NG	NG	NG	NG	NG	NG	NG
North G6	NG	NG	NG	NG	NG	NG	NG	NG	NG
North G8	NG	NG	NG	NG	NG	NG	NG	NG	NG
North G12	22	9,963	208	NG	NG	NG	NG	NG	NG
West F2	24	9,401	215	9	11,062	235	0	13,025	260
West F5	37	8,537	207	26	11,436	244	21	13,131	267
North I2	NG	NG	NG	NG	NG	NG	NG	NG	NG
North I5	NG	NG	NG	NG	NG	NG	NG	NG	NG
North I9	NG	NG	NG	NG	NG	NG	NG	NG	NG
North I13	23	7,945	209	NG	NG	NG	NG	NG	NG
West H2	24	9,896	213	14	12,053	240	5	12,823	250
West H4	17	10,300	216	8	13,000	245	2	14,411	260
East K1	5	8,949	197	NG	NG	NG	NG	NG	NG
East K4	18	9,535	210	6	11,595	237	NG	NG	NG
East O1	3	8,606	203	NG	NG	NG	NG	NG	NG
East O3	13	9,427	210	5	11,517	240	NG	NG	NG
East R3	14	9,549	205	9	12,919	257	6	13,967	273

Table 3. Three vitrinite reflectance values compared with age, depth, and temperature of gas generation in the Wilcox Formation in modeled Louisiana wells.

[R_o, vitrinite reflectance value—shown at top of Wilcox (*A*) and base of Wilcox (*B*); Ma, mega-annum; ft, foot; Temp. (F), temperature, degrees Fahrenheit; NG, no generation]

A.

Well	Top of Wilcox Formation, Louisiana								
	Start gas generation (R_o = 0.5)			Peak gas generation (R_o = 0.8)			End gas generation (R_o = 2.0)		
	Age (Ma)	Depth (ft)	Temp. (F)	Age (Ma)	Depth (ft)	Temp. (F)	Age (Ma)	Depth (ft)	Temp. (F)
North A11	NG	NG	NG	NG	NG	NG	NG	NG	NG
North C3	NG	NG	NG	NG	NG	NG	NG	NG	NG
North C7	NG	NG	NG	NG	NG	NG	NG	NG	NG
North C10	NG	NG	NG	NG	NG	NG	NG	NG	NG
West B2	12	6,847	179	NG	NG	NG	NG	NG	NG
West B6	35	6,962	188	14	12,683	264	NG	NG	NG
North E2	NG	NG	NG	NG	NG	NG	NG	NG	NG
North E7	NG	NG	NG	NG	NG	NG	NG	NG	NG
North E11	NG	NG	NG	NG	NG	NG	NG	NG	NG
North E14	NG	NG	NG	NG	NG	NG	NG	NG	NG
West D3	21	8,356	192	NG	NG	NG	NG	NG	NG
North G3	NG	NG	NG	NG	NG	NG	NG	NG	NG
North G6	NG	NG	NG	NG	NG	NG	NG	NG	NG
North G8	NG	NG	NG	NG	NG	NG	NG	NG	NG
North G12	NG	NG	NG	NG	NG	NG	NG	NG	NG
West F2	12	7,337	182	NG	NG	NG	NG	NG	NG
West F5	24	7,887	195	2	13,233	266	NG	NG	NG
North I2	NG	NG	NG	NG	NG	NG	NG	NG	NG
North I5	NG	NG	NG	NG	NG	NG	NG	NG	NG
North I9	NG	NG	NG	NG	NG	NG	NG	NG	NG
North I13	NG	NG	NG	NG	NG	NG	NG	NG	NG
West H2	12	7,932	185	NG	NG	NG	NG	NG	NG
West H4	21	8,653	191	NG	NG	NG	NG	NG	NG
East K1	NG	NG	NG	NG	NG	NG	NG	NG	NG
East K4	12	7,734	185	NG	NG	NG	NG	NG	NG
East O1	NG	NG	NG	NG	NG	NG	NG	NG	NG
East O3	8	7,942	191	NG	NG	NG	NG	NG	NG
East R3	12	9,160	199	0	13,629	267	NG	NG	NG

Table 3. Three vitrinite reflectance values compared with age, depth, and temperature of gas generation in the Wilcox Formation in modeled Louisiana wells.—Continued

[R_o, vitrinite reflectance value—shown at top of Wilcox (*A*) and base of Wilcox (*B*); Ma, mega-annum; ft, foot; Temp. (F), temperature, degrees Fahrenheit; NG, no generation]

B.

Well	Base of Wilcox Formation, Louisiana								
	Start gas generation (R_o = 0.5)			Peak gas generation (R_o = 0.8)			End gas generation (R_o = 2.0)		
	Age (Ma)	Depth (ft)	Temp. (F)	Age (Ma)	Depth (ft)	Temp. (F)	Age (Ma)	Depth (ft)	Temp. (F)
North A11	NG	NG	NG	NG	NG	NG	NG	NG	NG
North C3	NG	NG	NG	NG	NG	NG	NG	NG	NG
North C7	NG	NG	NG	NG	NG	NG	NG	NG	NG
North C10	NG	NG	NG	NG	NG	NG	NG	NG	NG
West B2	43	6,972	187	NG	NG	NG	NG	NG	NG
West B6	41	7,156	190	23	12,833	265	NG	NG	NG
North E2	NG	NG	NG	NG	NG	NG	NG	NG	NG
North E7	NG	NG	NG	NG	NG	NG	NG	NG	NG
North E11	30	5,555	178	NG	NG	NG	NG	NG	NG
North E14	41	6,649	183	NG	NG	NG	NG	NG	NG
West D3	39	7,311	183	14	13,825	265	NG	NG	NG
North G3	NG	NG	NG	NG	NG	NG	NG	NG	NG
North G6	NG	NG	NG	NG	NG	NG	NG	NG	NG
North G8	NG	NG	NG	NG	NG	NG	NG	NG	NG
North G12	36	7,713	183	NG	NG	NG	NG	NG	NG
West F2	33	7,069	185	NG	NG	NG	NG	NG	NG
West F5	45	6,898	183	22	12,930	265	NG	NG	NG
North I2	NG	NG	NG	NG	NG	NG	NG	NG	NG
North I5	NG	NG	NG	NG	NG	NG	NG	NG	NG
North I9	21	5,168	170	NG	NG	NG	NG	NG	NG
North I13	33	6,052	180	NG	NG	NG	NG	NG	NG
West H2	38	7,128	182	0	13,765	262	NG	NG	NG
West H4	23	8,800	200	NG	NG	NG	NG	NG	NG
East K1	22	8,011	185	NG	NG	NG	NG	NG	NG
East K4	24	8,161	193	NG	NG	NG	NG	NG	NG
East O1	16	7,199	186	NG	NG	NG	NG	NG	NG
East O3	20	7,336	185	NG	NG	NG	NG	NG	NG
East R3	15	8,732	197	7	13,736	269	NG	NG	NG

Source rock hydrous-pyrolysis kinetic parameters in combination with burial history reconstructions determine the timing and extent of oil generation and expulsion in the Wilcox Formation. In the present study, the generation of oil is defined by transformation ratios between 0.05 and 0.95. Immature source rocks in the Wilcox have ratios less than 0.05 and mature source rocks that have completed oil generation have ratios greater than 0.95. Peak oil generation is marked by a ratio of 0.50. There is a degree of uncertainty in the timing and extent of oil generation in some wells due to inconsistencies in the measured temperature data; nevertheless, the model results are internally consistent and agree with the geologic history of the region.

On the basis of model simulations, generation of oil commenced in the Wilcox during a fairly wide age range, 37 million years ago (Ma) to the present (fig. 9; table 2). The extent and timing of generation differs depending on the location of the well in the basin. In wells updip (north) of the Cretaceous shelf edge (North-A11, -C3, -C7, -C10, -E2, -E7, -E11, -G3, -G6, -G8, -I2, -I5, and -I9), the Wilcox is thermally immature at burial depths less than about 5,600 ft and has not generated oil. In contrast, close to the shelf edge (East-K1 and -O1, and North-E14, -G12, and -I13), oil was generated in and expelled from the lower part of the Wilcox Formation, but its levels of maturity were not sufficient to reach peak generation. Model simulations indicate that oil generation at the base of the Wilcox began in the early Miocene to Pliocene (≈23–3 Ma) along the shelf-edge in wells at depths of about 8,000 to 10,000 ft and temperatures approximating 200 to 210°F. Downdip (south) of the shelf edge (East-K4, -O3, and -R3, and West-B2, -B6, -D3, -F2, -F5, -H2, and -H4), oil generation at the base of the Wilcox commenced in the late Eocene to middle Miocene (≈37–13 Ma). The peak was reached in the late Oligocene to early Pliocene (≈27–5 Ma), and generation was completed in the late Miocene to the present (≈23–0 Ma). Burial temperatures at the onset of generation ranged from about 200 to 215°F at depths of approximately 8,300 to 9,900 ft and at the end of generation in most places (in the late Miocene) temperatures varied from about 250 to 270°F at depths of approximately 11,500 to 14,000 ft. In two wells (East-K4 and -O3), oil generation at the base of the Wilcox was not completed and may still be taking place today.

Model results indicate that generation of oil at the top of the Wilcox began in nine downdip wells (East-K4, -O3, and -R3, and West-B6, -D3, -F2, -F5, -H2, and -H4) but was completed in only three of them (East-R3, West-B6, and West-F5). In those nine wells, oil was generated from the Oligocene to the present (≈29–0 Ma), at temperatures of about 200 to 220°F and at depths of approximately 8,500 to 10,700 ft. Generation peaked in wells East-R3, West-B6, and West-F5 in the early to late Miocene (≈22–5 Ma) and was completed in the early Miocene to Pliocene (≈16–2 Ma). During peak generation, burial temperatures at the top of the Wilcox ranged from about 205 to 220°F at depths of approximately 8,500 to 10,700 ft; when generation ended, the temperatures ranged from about 250 to 265°F at depths of approximately 12,200 to 13,700 ft.

In two downdip wells (East-R3 and West-F5), maximum burial temperatures are about 265°F at the top of the Wilcox and exceed 300°F at the base of the formation. According to Hunt (1996), when generated oil in source rocks or in reservoirs reaches a temperature of 130°C (266°F) the oil begins to crack to gas; the cracking reaction is completed at 150 to 175°C (302–347°F). Temperatures corresponding to the onset of oil-to-gas cracking (130°C (≈265°F)) in wells East-R3 and West-F5 occur at burial depths of approximately 13,500 ft. It follows that at

depths and temperatures greater than 13,500 ft and 130°C (≈265°F), any oil generated from oil-prone source rocks in the Wilcox may have cracked to gas.

Gas generation in the Wilcox Formation, assuming the presence of adequate source facies, was evaluated on the basis of calculated R_o in conjunction with reconstructed burial-history curves (fig. 10, table 3). Generation of gas from Type III kerogen (not oil-cracking) is defined by R_o values between 0.5 and 2.0 percent. Immature (Type III) source rocks that have generated no gas have R_o values less than 0.5 percent, and mature source rocks that have completed gas generation have values greater than 2.0 percent. Peak gas generation corresponds to a R_o value of 0.8 percent. As a general rule, the onset of gas generation in the Wilcox was initiated earlier in the south where the source rocks were buried the deepest. On the basis of the model simulations, generation of gas occurred at the base of the Wilcox in only two updip wells (North-E11 and -I9). Generation commenced in late Oligocene to early Miocene time (≈30–20 Ma) at temperatures of about 170 to 180°F; burial depths ranged from approximately 5,200 to 5,600 ft. Model results indicate that gas was generated at the base of the Wilcox in all wells close to and downdip of the Lower Cretaceous shelf edge (East-K1 and -O1; North-E14, -G12, and -I13; East-K4, -O3, and -R3; West-B2, -B6, -D3, -F2, -F5, -H2, and -H4). Generation commenced in the middle Eocene to middle Miocene (≈45–15 Ma) at burial depths of approximately 6,000 to 8,800 ft and at temperatures from about 180 to 200°F. Peak generation was reached in the early Miocene to the present (≈23–0 Ma) in five downdip wells (East-R3; West-B6, -D3, -F5, and -H2) at burial depths of approximately 12,800 to 13,800 ft and temperatures of about 260 to 270°F. However, none of these wells reached a maximum maturity of 2.0 percent R_o.

Model results indicate that generation of gas at the top of the Wilcox Formation began in all 10 downdip wells (East-K4, -O3, and -R3; -B2, -B6, -D3, -F2, -F5, -H2, and -H4) but reached peak generation in only three wells (East-R3; WestB6 and -F5). Generation commenced in the early Oligocene to late Miocene (≈35–8 Ma) and peaked in the middle Miocene to the present (≈14–0 Ma). At the onset of generation, burial temperatures varied from about 180 to 200°F at depths of approximately 6,800 to 9,000 ft; during the time of peak generation, temperatures ranged from about 265 to 270°F at depths of approximately 12,700 to 13,600 ft.

Transformation Ratio Contours, Thermal Maturity, and Generation of Oil and Gas

The extent of thermal maturity and oil generation at the top and base of the Wilcox is represented as a series of transformation ratio contours (0.05, 0.50, and 0.95) in figure 11. Also shown are the distribution of Tertiary oils (Hood and others, 2002) and location of the Lower Cretaceous shelf edge. Source rocks that are thermally immature and have not generated oil (depths less than about 5,000 ft) lie updip of the 0.05 contour north of the shelf edge and source rocks that have generated all of their oil and are overmature (depths greater than ≈13,000 ft) are present south of the shelf edge, downdip of the 0.95 contour. Transformation ratio contours between 0.05 and 0.95 indicate mature source rocks where from 5 to 95 percent of the generation potential has been completed.

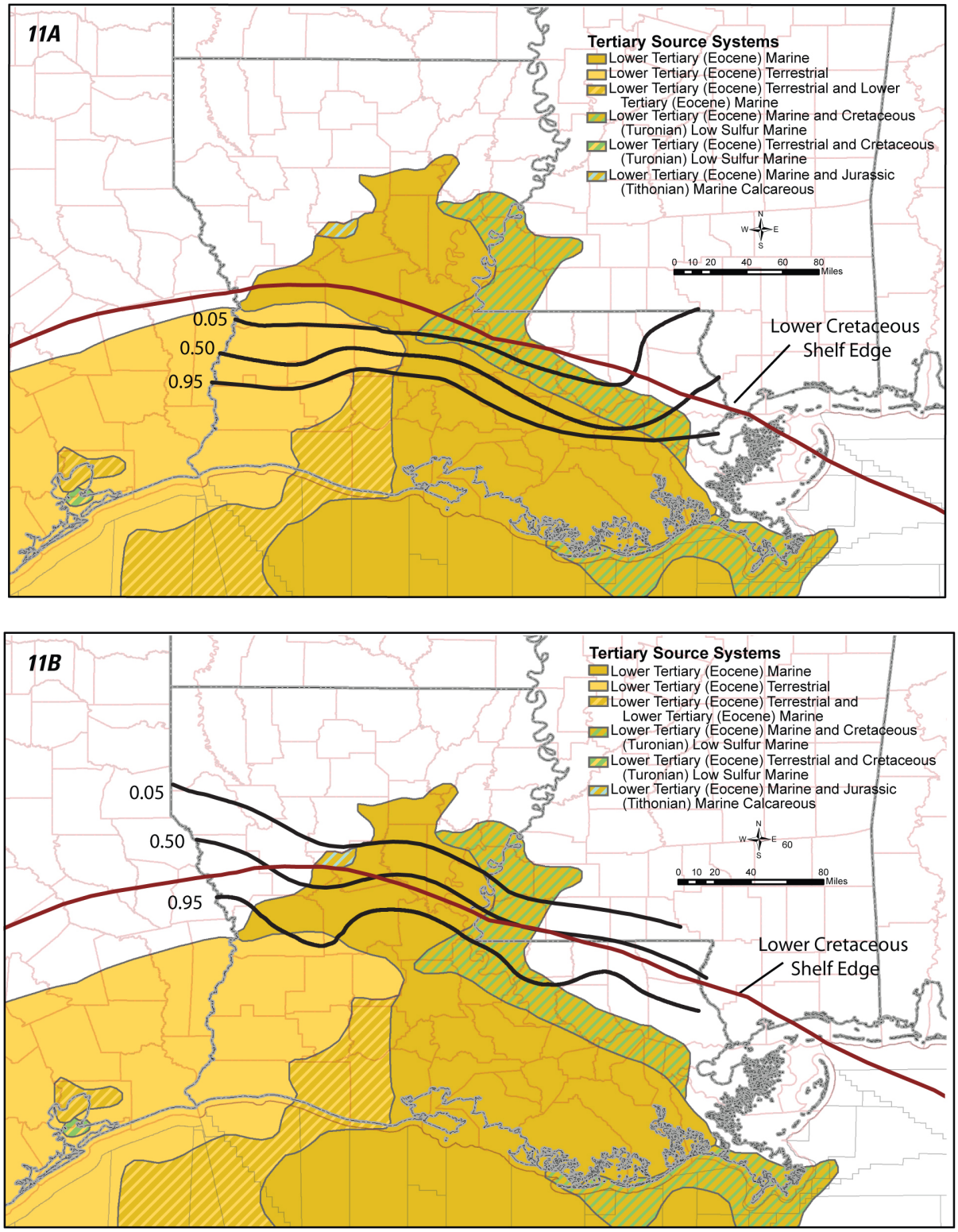

Figure 11. Northern Gulf Coast region showing extent of oil generation in the Wilcox Formation at top of Wilcox (*A*) and base of Wilcox (*B*). Lines show transformation ratios at start of oil generation (0.05), peak generation (0.50), and end of generation (0.95).

Differences in maturity with respect to oil generation across the shelf edge (fig. 11) may be related to the development of the carbonate shelf margin during the Early Cretaceous. The shelf margin is interpreted to have formed from a change in slope of the basement, which is marked by a crustal hinge zone, and from depositional patterns (Dobson, 1990; Sawyer and others, 1991). The hinge zone formed in response to differential subsidence across a boundary between thick and thin transitional crust (Corso, 1987) and was the site of substantial siliciclastic sedimentation from the Late Cretaceous through much of Cenozoic time (Salvador, 1991). High rates of sediment deposition coupled with increased accommodation space at the Cretaceous shelf margin led to deep burial of Cretaceous and Tertiary source rocks and, in turn, rapid generation of petroleum and cracking of oil to gas.

A number of studies document that the youngest oils in the Gulf Coast were derived from Cenozoic source rocks (Chinn and others, 1990; Cole and others, 1990; Hanor and Sassen, 1990; Sassen, 1990; Wenger and others, 1990; Kennicutt and others, 1992; Hood and others, 2002). However, geochemical analysis of oil extracts indicates that lignites, subbituminous coals, and shales in the Wilcox provided a large fraction of the oils in Oligocene and younger reservoirs (Sassen, 1990; Wenger and others, 1994; Hood and others, 2002). As a source rock, coal generally is thought to produce mostly gas; however, coals in the Wilcox generated abundant oil because the coals are of higher plant origin, thus contain hydrogen-rich (oil-prone) kerogen (Mukhopadhyay, 1989; Goddard, 1995). Eocene coals enriched in hydrogen can account for the Tertiary terrestrial-type oils in Texas and west-central Louisiana but they do not explain Tertiary marine oils that occur throughout much of eastern Louisiana. On the basis of oil source-rock correlations (Wenger and others, 1994; Hood and others, 2002), Tertiary marine oils extend from offshore Gulf of Mexico, across depositional facies of the Wilcox Formation, to north of the Cretaceous shelf margin (fig. 11). These oils may indicate a change from terrestrial to marine source facies; however, such a facies change is difficult to explain geologically, as no marine source rocks of Tertiary age have been observed onshore (although at burial depths greater than 25,000 ft, the Eocene section has not been penetrated). Another explanation is that the oils were derived from marine mudstones in the Sparta Formation, which overlies the Wilcox (fig. 3) and presumably has generated petroleum offshore where the stratigraphic section is deeply buried and mature. If we assume that this is the case, these oils may have migrated updip more than 80 miles from the nearest mature source and charged younger reservoirs. Migration of short- to long distances thus can account for the presence of Tertiary marine oil north of the Cretaceous shelf margin where model simulations indicate that Tertiary source rocks are immature. A similar interpretation based on geochemical data was presented by Sassen (1990) and Sassen and Chinn (1990).

Gas generation in the Wilcox Formation is represented by isoreflectance contours (0.5 and 0.8 percent R_o) in figure 12. As with the generation of oil, source rocks north of the 0.5 percent R_o contour are immature with respect to gas generation, and they have completed gas generation south of the 0.8 percent R_o contour. Peak gas generation occurs at 0.8 percent Ro; the end of gas generation (R_o = 2.0 percent) was not reached in the wells of the study. Unlike the sources of oil, the sources of gas in Paleogene and Neogene reservoirs cannot be identified with certainty.

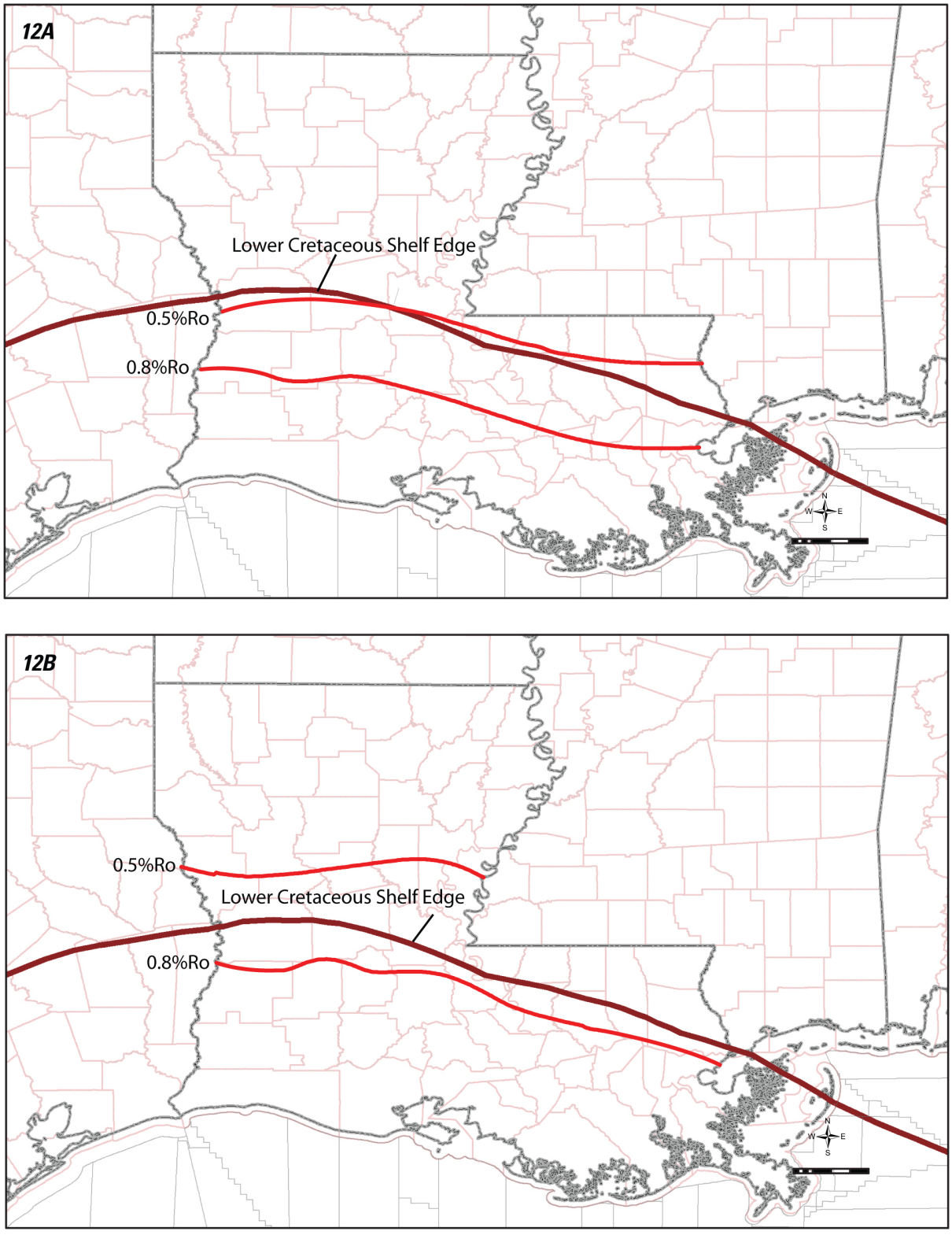

Figure 12. Northern Gulf Coast region showing extent of gas generation in the Wilcox Formation at top of Wilcox (*A*) and base of Wilcox (*B*). Lines show vitrinite reflectance (R_o) values at start of gas generation (0.5 percent R_o) and peak generation (0.8 percent R_o); end of generation (2.0 percent R_o) not reached in the wells studied.

Downdip of the Cretaceous shelf edge, at burial depths exceeding approximately 13,000 ft, maximum burial temperatures commonly exceed 266 to 347°C, which is the thermal range at which oil cracking occurs (Hunt, 1996). According to Henry and Lewan (2001), the amount of gas generated from the cracking of oil is 4 to 20 times as high as the amount generated from kerogen. This relation indicates that most of the gas associated with the Wilcox at depths greater than about 13,000 ft may result from oil-to-gas cracking rather than directly from kerogen.

References

Bebout, D.G., and Gutierrez, D.R., 1982, Regional cross sections, Louisiana Gulf Coast (western part): Louisiana Geological Survey Folio Series 5, 12 p.

Bebout, D.G., and Gutierrez, D.R., 1983, Regional cross sections, Louisiana Gulf Coast (eastern part): Louisiana Geological Survey Folio Series 6, 10 p.

Blackwell, D.D., and Richards, M.C., 2004, Geothermal map of North America: American Association of Petroleum Geologists, scale 1:6,500,000. *http://bookstore.aapg.org/*

Chinn, E.W., Cole, G.A., Gibbons, M.J., Sassen, R., and Drozd, R.J., 1990, Organic geochemistry of lower Tertiary shales of southern Louisiana [abs.]: American Association of Petroleum Geologists Bulletin, v. 74, p. 630.

Cole, G.A., Chinn, E.W., Pigott, N., Gibbons, M.J., and Sassen, R., 1990, Origin of Tertiary reservoired hydrocarbons along the central Texas and Louisiana Gulf Coast rim [abs.]: American Association of Petroleum Geologists Bulletin, v. 74, p. 68. Corso, W., 1987, Development of the Early Cretaceous northwest Florida carbonate platform: Austin, The University of Texas, PhD. dissertation, 165 p.

Dobson, L.M., 1990, Seismic stratigraphy and geologic history of Jurassic rocks, northeastern Gulf of Mexico: Austin, The University of Texas, M.S. thesis, 165 p.

Driskill, B.W., Nunn, J.A., Sassen, R., and Pilger, Jr., R.H., 1988, Tectonic subsidence, crustal thinning, and petroleum generation in the Jurassic trend of Mississippi, Alabama, and Florida: Gulf Coast Association of Geological Societies Transactions, v. 38, p. 257–265.

Eversull, L.G., 1984, Regional cross sections, Louisiana Gulf Coast (northern part), Louisiana Geological Survey Folio Series 7, 12 p.

Goddard, D., 1995, Deltaic reservoir characterization—Geological, petrophysical, and engineering applications: Basin Research Institute Technical Report, 125 p.

Hanor, J.S., and Sassen, R., 1990, Evidence for large-scale vertical and lateral migration of formation waters, dissolved salt, and crude oil in the Louisiana Gulf Coast, *in* Schumacher, D., and Perkins, B.F., eds., Gulf Coast oil and gases: Annual Research Conference of the Gulf Coast Section of the SEPM Foundation, 9th, Proceedings: p. 283–296.

Henry, A.A., and Lewan, M.D., 2001, Comparison of kinetic-model predictions of deep gas generation, *in* Dyman, T.S., and Kuuskraa, V.A., eds., Geologic studies of deep natural gas resources: U.S. Geological Survey Digital Data Series 67, chap. D, CD ROM.

Hermanrud, C., 1993, Basin modeling techniques—An overview, *in* Doré, A.G., Auguston, J.H., Hermanrud, C., Stewart, D.S., and Sylta, O., eds., Basin modelling—Advances and applications: Norwegian Petroleum Society (NPF) Special Publication 3, p. 1–34.

Hood, K.C., Wenger, L.M., Gross, O.P., and Harrison, S.C., 2002, Hydrocarbon systems analysis of the northern Gulf of Mexico—Delineation of hydrocarbon migration pathways using seeps and seismic imaging, *in* Schumacher D., and LeSchack, L.A., eds., Surface exploration case histories—Applications of geochemistry, magnetics, and remote sensing: American

Association of Petroleum Geologists Studies in Geology 48 and SEG Geophysical Reference Series 11, p. 25–40.
Hunt, J., 1996, Petroleum geochemistry and geology (2d ed.): New York, W.H. Freeman and Company, 743 p.
Hunt, J.M., Lewan, M.D., and Hennet, R.J.-C., 1991, Modeling oil generation with time-temperature index graphs based on the Arrhenius equation: American Association of Petroleum Geologists Bulletin, v. 75, no. 4, p. 795–807.
Keen, C.E., and Lewis, T., 1982, Measured radiogenic heat production in sediments from continental margin of eastern North America—Implications for petroleum generation: American Association of Petroleum Geologists Bulletin, v. 66, p. 1402–1407.
Kennicutt, M.C., II, McDonald, T.J., Comet, P.A., Denoux, G.J., and Brooks, J.M., 1992, The origins of petroleum in the northern Gulf of Mexico: Geochimica Cosmochimica Acta, v. 56, p. 1259–1280.
Kotarba, M.J., and Lewan, M.D., 2004, Characterizing thermogenic coalbed gas from Polish coals of different rank by hydrous pyrolysis: Organic Geochemistry, v. 35, p. 615–646.
Lewan, M.D., and Ruble, T.E., 2002, Comparison of petroleum generation kinetics by isothermal hydrous and non-isothermal open-system pyrolysis: Organic Geochemistry, v. 33, p. 1457–1475.
Martin, R.G., 1978, Northern and eastern Gulf of Mexico continental margin—Stratigraphic and structural framework: American Association of Petroleum Geologists Bulletin, v. 7, p. 21–42.
McDade, E.C., 2002, Organic-rich lower Tertiary shales, south Louisiana—Implications for petroleum source rock deposition: Baton Rouge, Louisiana State University, PhD. dissertation, 248 p.
McDade, E.C., Sassen, R., Wenger, L., and Cole, G.A., 1993, Identification of organic-rich lower Tertiary shales as petroleum source rocks, South Louisiana: Gulf Coast Association of Geological Societies Transactions, v. 43, p. 257–267.
McKenna, T.E., and Sharp, J.M., Jr., 1998, Radiogenic heat production in sedimentary rocks of the Gulf of Mexico Basin (south Texas): American Association of Petroleum Geologists Bulletin, v. 82, p. 484–496.
Morton, R.A., Gordon, P.T., Foote, R.O., Massingill, L.M., 1990, Gulf Coast regional cross section—Texas lower coastal plain—offshore sector: American Association of Petroleum Geologists Map, sheet 3 of 3.
Mukhopadhyay, P.K., 1989, Organic petrography and organic geochemistry of Texas Tertiary coals in relation to depositional environment and hydrocarbon generation: The University of Texas at Austin Bureau of Economic Geology Report of Investigations, v. 188, 118 p.
Negraru, P.T., Blackwell, D.D., and Erkan, K., 2004, Heat flow in Texas: American Association of Petroleum Geologists Annual Meeting, Dallas, Texas, April 18–21, 2004, Abstract Volume: American Association of Petroleum Bulletin, v. 13, p. A104.
Nunn, J.A., and Sassen, R., 1986, The framework of hydrocarbon generation and migration, Gulf of Mexico continental slope: Gulf Coast Association of Geological Societies Transactions, v. 36, p. 257–262.
Pepper, A.S., and Corvi, P.J., 1995, Simple kinetic models of petroleum formation, part I—Oil and gas generation from kerogen: Marine and Petroleum Geology, v. 12, p. 291–319.
Roberts, L.N.R., Lewan, M.D., and Finn, T.M., 2004, Timing of oil and gas generation of petroleum systems in the southwestern Wyoming province: The Mountain Geologist, v. 41, no. 3, p. 87–118.

Ruble, T.E., Lewan, M.D., and Philip, R.P., 2001, New insights on the Green River petroleum system in the Uinta Basin from hydrous pyrolysis experiments: American Association of Petroleum Geologists Bulletin, v. 85, no. 8, p. 1333–1371.
Salvador, A., 1987, Late Triassic-Jurassic paleogeography and origin of Gulf of Mexico Basin: American Association of Petroleum Geologists Bulletin, v. 71, p. 419–451.
Salvador, A., 1991, The Gulf of Mexico Basin, *in* Salvador, A., ed., The Gulf of Mexico Basin—The Geology of North America, The Gulf of Mexico: The Decade of North American Geology (DNAG): Geological Society of America, v. J, 568 p.
Salvador, A., and Muneton, J.M.Q., 1991, Stratigraphic correlation chart, Gulf of Mexico Basin, *in* Salvador, A., ed., The Geology of North America, The Gulf of Mexico: The Decade of North American Geology (DNAG): Geological Society of America, v. J, plate 5, 1 sheet.
Sassen, R., 1990, Lower Tertiary and Upper Cretaceous source rocks in Louisiana and Mississippi—Implications to Gulf of Mexico crude oil: American Association of Petroleum Geologists Bulletin, v. 74, p. 857–878.
Sassen, R., and Chinn, E.W., 1990, Implications of lower Tertiary source rocks in south Louisiana to the origin of Gulf of Mexico crude oil, offshore Louisiana, *in* Gulf Coast Section of the SEPM, Bob F. Perkins Research Conference, 9th, p. 175–179.
Sassen, R., Tye, R.S., Chinn, E.W., and Lemoine, R.C., 1988, Origin of crude oil in the Wilcox trend of Louisiana and Mississippi—Evidence for long range migration: Gulf Coast Association of Geological Societies Transactions, v. 38, p. 27–34.
Sawyer, D.S., Buffler, R.T., and Pilger, R.H., Jr., 1991, The crust under the Gulf of Mexico, *in* Salvador, A., ed., The Gulf of Mexico Basin: Geological Society of America, The Decade of North American Geology (DNAG), v. J, p. 53–72.
Smith, D.L., Dees, W.J., and Harrelson, D.W., 1981, Geothermal conditions and their implications for basement tectonics in the Gulf Coast margin: Gulf Coast Association of Geological Societies Transactions, v. 31, p. 181–190.
Stoudt, D.L., Hutchinson, P.J., and Gordon, P.T., 1990a, Gulf Coast regional cross section—East Texas–Texas Coastal Plain Sector: American Association of Petroleum Geologists Map, Sheet 2 of 3.
Stoudt, D.L., McCulloh, R.P., and Eversull, L.G., 1990b, Gulf Coast regional cross section—Southwest Arkansas-Northwest Louisiana Sector: American Association of Petroleum Geologists Map, Sheet 1 of 3.
Sweeney, J.J., and Burnham, A.K., 1990, Evaluation of a simple model of vitrinite reflectance based on chemical kinetics: American Association of Petroleum Geologists, v. 74, p. 1559–1570.
Tang, Y., Jenden, P.D., Nigrini, A., and Teerman, S.C., 1996, Modeling early methane generation in coal: Energy and Fuels, v. 10, p. 659–671.
U.S. Geological Survey, 2007, Assessment of undiscovered oil and gas resources in Tertiary strata of the Gulf Coast: U. S. Geological Survey Fact Sheet 3146, 2 p.
Wenger, L.M., Goodoff, L.R., Gross, O.P., Harrison, S.C., and Hood, K.C., 1994, Northern Gulf of Mexico—An integrated approach to source, maturation, and migration, *in* Scheidermann, N., Cruz, P., and Sanchez, R., eds., Geologic aspects of petroleum systems: Joint American Association of Petroleum Geologists–AMGP Hedberg Research Conference, 1st, Proceedings, 5 p.
Wenger, L.M., Sassen, R., and Schumacher, S., 1990, Molecular characteristics of Smackover-, Tuscaloosa- and Wilcox-reservoired oils in the eastern Gulf Coast, *in* Schumacher D., and

Perkins, B.F., eds., Gulf Coast Oil and Gases, Annual Research Conference of the Gulf Coast Section of the SEPM Foundation: 9th, Proceedings: p. 37–57.
Wygrala, B.P., 1989, Integrated study of an oil field in the southern Po Basin, northern Italy: Berichte der Kernforschungsanlage Julich, 2313, ISSN 0366–0885, 217 p.